学位論文

Studies of vacuolar trafficking pathways regulated by RAB5 and RAB7 in *Arabidopsis thaliana*

（シロイヌナズナにおける RAB5 と RAB7 が制御する液胞輸送経路の研究）

平成 25 年 12 月博士（理学）申請

東京大学大学院理学系研究科

生物科学専攻

井上 丈司

Table of Contents

Acknowledgements

First of all, I wish to express my appreciation to my supervisor, associate professor Takashi Ueda, University of Tokyo, for his supervision and encouragement throughout this study.

I also thank Gorou Horiguchi (Rikkyo University), Renze Heidstra (Wageningen University), Philip Benfey (Duke University), Thomas Laux (University of Freiburg), Ben Scheres (Wageningen University), Jiri Friml (Ghent University), Masatoshi Yamaguchi (Saitama University), and Taku Demura (NAIST), Miyo Terao-Morita (Nagoya University), Shigeru Utsumi (Kyoto University) and Ikuko Hara-Nishimura (Kyoto University) sharing materials. I thank for E. Furuyama (University of Tokyo), W. Uchida (RIKEN), Y. Ichikawa (RIKEN), R. Nakazawa (RIKEN), and S. Fukushima (RIKEN) for technical support; C. Ungermann (University of Osnabrück) for precious advice about the GEF assay; and the SALK Institute, the Max Planck Institute, and the ABRC for providing *Arabisospsis thaliana* mutants.

I also thank Kazuo Ebine, Yuki Kondo, Satoshi Naramoto, Jun Ito, Emi Ito, Tomohiro Uemura, Tatsuaki Goh, Hiroshi Abe, Ken Sato and Akihiko Nakano for sharing materials, collaborative works and valuable discussion. I appreciate to all lab members for valuable discussion and technical supports.

Abstract

Eukaryotic cells embrace a variety of membrane-bound organelles with distinct functions, which rely on specific sets of proteins and lipids. Membrane trafficking is responsible for the specific localization of proteins in respective compartments. RAB GTPases regulate tethering and fusion of transport vesicles to target membranes in membrane trafficking by acting as molecular switches, cycling between GDP- and GTP-bound states. The multifunctional vacuole is the largest organelle in plant cells, and many proteins are transported to and stored in this organelle; thus, the vacuole has great physiological and agronomical importance. RAB5 and RAB7 are evolutionarily conserved subfamilies of RAB GTPase, whose animal and yeast counterparts regulate the vacuolar/endosomal trafficking in a sequential manner. In animal cells, RAB5 has been shown to perform various functions in the endocytic pathway, including the regulation of endosomal fusion and motility. RAB5-mediated endosomal trafficking has also been found to play important roles in various higher-order plant functions, which include the regulation of the polar transport of auxin and responses to environmental conditions. The regulatory mechanisms and functions of plant RAB5 have also been investigated at the molecular and cellular levels. However, the significance of RAB5 activity at the tissue and organ levels has hardly been investigated thus far. In Chapter 1,

I examined the effect of a mutation in *VPS9a*, which encodes the sole guanine nucleotide exchange factor (GEF) for all RAB5s in the vegetative stages of *Arabidopsis thaliana*. I found that multiple developmental processes were impaired in the mutant plants, including the growth and pattern formation of the roots and establishment of auxin maxima. My results indicate that RAB5 plays distinctive pivotal roles in the development of plants. In Chapter 2, I demonstrate that multiple vacuolar trafficking pathways operate in plants, which are distinctly regulated by RAB5 and RAB7. Functional analyses of an activating complex for RAB7 indicated that this complex is responsible for maturation from RAB5- to RAB7-positive endosomes, which suggested that plants are also equipped with the vacuolar trafficking pathway involving both RAB5 and RAB7. However, I also found that impairment of RAB5- and RAB7-dependent pathways differentially affected the transport of distinctive cargos, indicating that these machinery components are recruited to a more complex trafficking network in plants. These results indicate that plants have developed a complex vacuolar transport system distinct from that of non-plant systems by assigning evolutionarily conserved machineries to unique trafficking pathways, which provide a fundamental basis for plant development at the cellular and higher-ordered levels.

General Introduction

Eukaryotic cells contain a variety of membrane-bound organelles, which fulfill distinct functions through their specific protein contents. Membrane trafficking enables the proteins to localize on specific compartments. For example, plant vacuoles have multiple functions including the storage of nutrients and increase of cell volume, which rely on proteins in or on vacuoles such as seed storage proteins and aquaporins. Transport of proteins to the target organelles consists of following steps: budding of transport vesicles from a donor compartment, delivery of the transport vesicles, and tethering and fusion of the vesicles to a target compartment. RAB GTPase is a key regulator of the last step. RAB GTPase acts as a molecular switch by cycling between the active GTP-bound and inactive GDP-bound states. For activation of RAB GTPase, GDP on RAB GTPase must be replaced by GTP. This reaction is mediated by the specific guanine nucleotide exchange factor (GEF). *Arabidopsis thaliana* harbors 57 RAB GTPases, which are divided into eight subgroups (Saito and Ueda 2009). RAB5 and RAB7 subgroups are considered to act in endocytic and vacuolar transport pathways. The RAB5 group in land plants are further divided into two groups; in addition to the RAB5 orthologs, plants harbor the plant-specific type of RAB5, the ARA6 group (Ebine and Ueda 2009, Ueda *et al.* 2004, Ueda *et al.* 2001). There are

three RAB5-related proteins encoded in the *A. thaliana* genome: ARA7 and RHA1 (also known as RABF2b and RABF2a, respectively), conventional RAB5s, and ARA6 (also known as RABF1), the plant-unique RAB5. Recently, it was demonstrated that ARA6 acts in a different trafficking pathway than conventional RAB5 members; ARA6 regulates the trafficking pathway from endosomes to the plasma membrane, whereas conventional RAB5s function in the transport to vacuoles in endocytic and vacuolar trafficking pathways (Ebine *et al.* 2011). Despite the distinct functions of conventional and plant-unique RAB5 GTPases, these two groups share the common activator, VPS9a in *A. thaliana* (Goh *et al.* 2007).

The functions of RAB5 groups have been elucidated at the molecular and cellular levels. However, detailed analyses of the RAB5 functions at the tissue and organ levels have not yet been performed. In Chapter 1, I examined the phenotypes of the *vps9a*-2 mutant, a weak allele of the RAB5 GEF, and demonstrated that RAB5 activation is required for multiple steps of root development including cell division, cell elongation, cell morphogenesis, radial patterning of the root cell layers, and positioning of the auxin maxima in *A. thaliana*.

Regarding *A. thaliana* RAB7, its functions at the cellular level still remain elusive. In animal cells, the trafficking pathway from the early to late endosome is

regulated by a sequential action of RAB5 and RAB7, which is mediated by VPS39, a subunit of the HOPS complex (Rink *et al.* 2005) and the GEF for RAB7 consisting of SAND1/Mon1 and CCZ1a (Bohdanowicz and Grinstein 2010). The sequential interaction of these proteins and RAB GTPases is responsible for the maturation from early to late endosomal compartments (Kinchen and Ravichandran 2010, Poteryaev *et al.* 2010). Conversely, it is not clear how the vacuolar trafficking pathway is mediated by RAB5 and RAB7 in plant cells. In Chapter 2, I investigated involvement of RAB5 and RAB7 in vacuolar transport of some soluble and membrane proteins in *A. thaliana*. My research revealed that *A. thaliana* is equipped with the vacuolar trafficking pathway involving the sequential action of RAB5 and RAB7, and also harbors a unique trafficking pathway to the vacuole, which is independent of RAB7.

Chapter 1

RAB5 Activation is Required for Multiple Steps in *Arabidopsis thaliana* Root Development

Introduction

Recent studies of endosomal trafficking in plants have demonstrated its critical roles in various plant functions. For example, a guanine nucleotide exchange factor (GEF) for ARF GTPase, GNOM, is responsible for the endocytic recycling of an auxin efflux carrier, PIN1, which is essential for proper polar localization of PIN1 (Geldner *et al.* 2003). Endosomal trafficking has also been shown to be involved in responses to extracellular stimuli. The boron transporter BOR1 is internalized by endocytosis under high boron conditions for homeostasis of the plant nutrients (Takano *et al.* 2005). FLS2, an LRR receptor-like kinase that mediates defenses against bacterial pathogens, undergoes ligand-induced endocytosis (Beck *et al.* 2012, Robatzek *et al.* 2006). The endosomal system also plays essential roles in the biosynthetic trafficking pathway to the vacuole, which is also crucial for plant development (De Marcos Lousa *et al.* 2012, Mo *et al.* 2006, Rojo *et al.* 2001). It has been also shown that a plant-specific RAB5 GTPase, ARA6, is required for normal salinity stress tolerance (Ebine *et al.* 2011). Thus, endosomal trafficking plays fundamental roles in various functions of plants.

RAB GTPases are key molecules in the regulation of the tethering and/or fusion steps of transport vesicles to target membranes. Among RAB GTPases, animal RAB5 has been shown to perform various functions in the endocytic pathway, which

includes the regulation of homotypic early endosomal fusion, endosomal motility, and endosomal signaling (Grosshans *et al.* 2006). RAB5 is one of the conserved RAB GTPases that are predicted to exist in the common ancestor of all eukaryotic cells (Field *et al.* 2007, Pereira-Leal 2008), and all plant genomes that have been sequenced harbor *RAB5* orthologs; the unicellular red alga *Cyanidioschyzon merolae* is the only exception (Matsuzaki *et al.* 2004). Specific secondary loss of the RAB5-related machinery is suggested in this organism. In addition to the RAB5 orthologs, plants harbor another type of RAB5, the ARA6 group (Ebine and Ueda 2009, Ueda *et al.* 2004, Ueda *et al.* 2001). Three RAB5-related proteins are encoded in the *Arabidopsis thaliana* genome: ARA7 and RHA1 (also known as RABF2b and RABF2a, respectively), conventional RAB5s, and ARA6 (also known as RABF1), the plant-unique RAB5. Recently, ARA6 was shown to act in a different trafficking pathway than conventional RAB5 members; ARA6 regulates the trafficking pathway from endosomes to the plasma membrane by mediating the assembly of a distinctive SNARE complex at the plasma membrane, whereas conventional RAB5s function in the transport to vacuoles in endocytic and vacuolar transport pathways (Ebine *et al.* 2011).

RAB GTPases act as a molecular switch by cycling between the active GTP-bound and inactive GDP-bound states; GDP must be replaced by GTP to activate

RAB proteins. This reaction is mediated by the specific GEF. Despite the distinct functions of conventional and plant-unique RAB5 GTPases, these two groups share the same upstream regulator. *A. thaliana* VPS9a, which consists of the conserved VPS9a domain that catalyzes nucleotide exchange (Goh *et al.* 2007, Uejima *et al.* 2010, Uejima *et al.* 2013) and the plant-specific C-terminal domain, is responsible for nucleotide exchange on both conventional and plant-unique RAB5 proteins. The *A. thaliana* genome contains another gene encoding a VPS9 domain-containing protein, VPS9b, but *VPS9b* expression is not detected in vegetative tissues. Thus, VPS9a is practically the sole GEF for RAB5s in vegetative developmental stages in *A. thaliana* (Goh *et al.* 2007). Both ARA7 and ARA6 mislocalized in the cytosol of a null mutant of *VPS9a*, *vps9a-1* (Goh *et al.* 2007), like GDP-fixed mutants of ARA7 and ARA6 (Ebine and Ueda, unpublished result). Thus, two different RAB5 groups are regulated by the same activating factor in plants. In contrast, several distinct RAB5 GEFs function in different trafficking steps in the endocytic pathway in animal cells, which harbor only conventional RAB5. The difference in the upstream regulatory systems of RAB5 between plants and animals strongly suggests that plants and animals followed distinct evolutionary paths for modifying their RAB5-mediated trafficking pathways.

As mentioned above, the functions of RAB5 groups have been investigated

intensively at the molecular and cellular levels. However, detailed analyses of the significance of RAB5 function at the tissue and organ levels have not yet been performed, mainly because of a lack of a suitable experimental system for studying the tissue- or organ-level effects of the perturbation of RAB5 functions. All three RAB5 single mutants, *ara7*, *rha1*, and *ara6,* exhibit the indistinguishable phenotypes of wild-type plants, and the double mutant *ara7rha1* exhibits gametophytic lethality. The complete loss of function of *VPS9a* and over-expression of dominant negative ARA7 have also been shown to result in embryonic lethality (Dhonukshe *et al.* 2008, Goh *et al.* 2007). To overcome this problem, I used the *vps9a-2* mutant, a weak mutant allele that exhibits leaky phenotypes in multiple developmental stages, including root development (Goh *et al.* 2007). Using *vps9a-2* mutant plants, I examined the physiological significance of RAB5 activation in plant development. My results indicate that proper activation of RAB5 is required in various aspects of plant development, including cell division, cell elongation, cell morphogenesis, radial patterning of the root cell layers, and positioning of the auxin maxima in *A. thaliana*.

Results

Proper activation of RAB5 is required for root apical meristem activity and cell elongation in root development

It was previously shown that the *vps9a-2* mutant is defective in root development; the length of mutant roots was significantly shorter than that of wild-type roots (Goh *et al.* 2007). This phenotype could be accounted for by defective cell division in the root apical meristem (RAM) of mutant roots and/or impaired cell elongation. To verify these possibilities, I first observed the boundary between the division and elongation zones of the mutant roots, and found that the meristem region of the mutant root was smaller than that of the wild-type (Figure 1a,b). Next, I examined the expression of *cyc1At::GUS*, which is expressed in the G2/M phase transition and used as a marker of mitotic cells (Ferreira *et al.* 1994), in the root tips of wild-type and *vps9a-2* mutant plants. The number of GUS-stained cells in the mutant root tips was substantially lower than that of wild-type roots (Figure 1c, d). These results indicate that RAB5 activation is required for maintaining RAM activity.

I also examined whether the *vps9a-2* mutation exerted a deleterious effect on cell elongation. Because the root epidermal cells of the mutant were swollen and exfoliated from each other, making it difficult to measure their precise length (Figure 2),

I compared the length of endodermal cells at the boundary between the elongation and differentiation zones in wild-type and mutant plants. The length of mutant endodermal cells was significantly shorter than the length of wild-type endodermal cells (n = 20 roots; P <0.01, Student's *t* test; Figure 1e-g), indicating defective cell elongation in the mutant plants. Thus, proper activation of RAB5 is required for controlling both RAM activity and cell elongation in the *A. thaliana* root.

RAB5 activation is required for suppressing cell division in root cell layers

The root tips of young *A. thaliana* seedlings have four concentric cell layers outside the stele: the outermost lateral root cap, epidermis, cortex, and innermost endodermis. In wild-type *A. thaliana*, each of these tissues consists of a single cell layer (Figure 3a) (Benfey and Scheres 2000). In contrast, young *vps9a-2* seedlings exhibited four or more layers surrounding the stele (Figure 3b). The *vps9a-2* mutation also affected the cell number in each of these cell layers; the number of cells comprising endodermis, cortex, and epidermis of the *vps9a-2* roots were increased compared with the wild-type plant (Figure 3b). To determine the identity of the extra cell layers in the *vps9a-2* mutant, I introduced *pEn7::YFP*$_{H2B}$ or *pCo2::YFP*$_{H2B}$ into the mutant. *pEn7*::*YFP*$_{H2B}$ is highly expressed in the endodermal cells, and *pCo2*::*YFP*$_{H2B}$ is used as

a reporter of cortical cells (Figure 3c-f) (Heidstra *et al.* 2004). Observation of the roots transformed with these markers revealed that the increase in cell layers in mutant roots was caused by periclinal divisions of endodermal cells (Figure 3g,h). The outer daughter cells of divided endodermal cells also gradually lost endodermal identity, acquiring cortical identity (Figure 3i,j). The periclinal divisions and shift in identity have also been reported to occur in mature wild-type roots (Paquette and Benfey 2005), resulting in middle cortex formation. I quantified the middle cortex formation in 3-day-old roots, which indicated that the frequency of middle cortex formation is significantly elevated in the *vps9a-2* mutant compared to the wild-type (n = 3 experiments, 10 roots per experiment; $P < 0.05$, Student's *t* test; Figure 3k). I also observed that some of the inner daughter cells in mutant roots further divided periclinally (Figure 4). These results indicate that VPS9a is required to repress middle cortex formation at the premature stage in root development. It has been shown that middle cortex formation is under regulation of a plant hormone, gibberellin (Paquette and Benfey 2005). To examine the relationship between VPS9a and gibberellin in middle cortex formation, I then examined the effect of a gibberellin biosynthesis inhibitor, paclobutrazol (PAC), on periclinal division in roots of the *vps9a-2* mutant. By PAC treatment, frequency of middle cortex formation was significantly elevated in wild-type roots (n = 3

experiments, 10 roots per experiment; P <0.05, Student's *t* test; Figure 3k) as reported previously (Paquette and Benfey 2005). In contrast, significant difference in the rate of periclinal division was not observed between PAC-treated and untreated roots of the *vps9a-2* mutant (Figure 3k). This result may indicate that VPS9a regulates periclinal division of the root in the genetic framework that also involves gibberellin biosynthesis or gibberellin signaling.

Expression patterns of *SHR* and *SCR* were affected by *vps9a-2*

Similar abnormalities in the root radial patterning as what was observed in *vps9a-2* roots have been observed when *SHORT-ROOT* (*SHR*) is over-expressed or ectopically expressed or *SCARECROW (SCR)* expression is decreased (Cui *et al.* 2007, Helariutta *et al.* 2000, Nakajima *et al.* 2001, Sena *et al.* 2004). Therefore, I examined whether the expression patterns of these genes are somehow affected in the primary roots of the *vps9a-2* mutant using reporter genes *pSHR::GFP* and *pSCR::GFP*. In wild-type plants transformed with *pSHR::GFP*, fluorescence was observed only in the stele, as reported previously (Figure 5a) (Helariutta *et al.* 2000). In the *vps9a-2* mutant, *SHR* expression expanded to the quiescent center (QC) and columella stem cells (CSC) in addition to the stele (Figure 5b). When expressing *pSCR::GFP*, I detected

fluorescence in all cells constituting the endodermis, QC, and cortical endodermal initial (CEI), as reported previously (Figure 5c) (Wysocka-Diller *et al.* 2000). However, in the *vps9a-2* mutant, loss of *pSCR::GFP* expression was observed frequently in QC and CEI (Figure 5d). I also observed that a part of the endodermal tissue in *vps9a-2* roots did not express *pSCR::GFP* (Figure 6). Thus, proper RAB5 activation is required for the establishment of *SHR* and *SCR* expression patterns in the root stem cell niche, and aberrations can result in abnormal radial patterning of the roots.

RAB5 activation is not required for QC identity

The abnormal *SHR* and *SCR* expression patterns in QC implied that the identity of QC cells was partly compromised and that they acquired some of the characteristics of the stele in *vps9a-2* because the stele in wild-type roots expressed *SHR* but not *SCR*. To verify this possibility, I investigated whether three QC identity markers, *pWOX5::GFP*, *QC46::GUS*, and *QC184::GUS*, were properly expressed in the *vps9a-2* mutant (Sabatini *et al.* 1999, Sarkar *et al.* 2007). Unexpectedly, I did not see any difference in the patterns of GFP fluorescence and GUS staining between wild-type and mutant roots (Figure 5e-j). Next, I examined the expression of *pVND3::YFP-nuc*, a marker expressed in the procambium tissue (Kubo *et al.* 2005), in the *vps9a-2* mutant. I

did not observe YFP fluorescence in the QC cells of *vps9a-2* plants, which strongly suggests that the QC did not bear the procambial character (Figure 7). These results indicate that the QC in the mutant plants acquired its appropriate identity, at least partly, but it lacked *SCR* expression and ectopically expressed *SHR*.

Positioning of the auxin response maxima depends on RAB5 activation

To further characterize the QC in *vps9a-2* plants, I examined the auxin responsive pattern in mutant roots. The auxin response maxima in roots are reported to be located at the QC, which is required for specification of the QC identity (Blilou *et al.* 2005, Sabatini *et al.* 1999, Ulmasov *et al.* 1997). Using the *pDR5::GFP* reporter gene, I monitored the distribution of the auxin response in *vps9a-2* plants exhibiting abnormal expression patterns of *SHR* and *SCR* around the QC. As previously reported, the highest *pDR5::GFP* expression was observed at the QC in wild-type plants (Figure 8a). In *vps9a-2* plants, the auxin response maxima shifted downwards to the root caps (Figure 8b-d). This result indicates that RAB5 activation is required for positioning the auxin response maxima. I also noticed that the pattern of the auxin response in the stele was changed in *vps9a-2* plants. In the stele of the wild-type root, GFP fluorescence was apparent in all cells of the protoxylem and metaxylem cell layers above the QC cells. In

contrast, GFP fluorescence was absent in parts of the protoxylem and metaxylem cell files in *vps9a-2* plants (Figure 10). Thus, the auxin response was broadly disrupted in *vps9a-2* mutant roots, indicating important roles of RAB5 in determining and/or maintaining the auxin response maxima in roots, similar to the case in developing embryos (Dhonukshe *et al.* 2008).

RAB5 activation is required for the transport of PIN2 into the vacuole

Modulation of the auxin distribution is mediated by PIN proteins, some of which localize to the plasma membrane with clear polarity (Blilou *et al.* 2005). Impaired positioning of the auxin response maximum in the mutant raised the possibility that the *vps9a-2* mutation also affects the expression or localization of PIN proteins. To verify this possibility, I examined the expression pattern and localization of PIN2-GFP, the expression of which was driven by its own promoter. Though the expression pattern in *vps9a-2* plants was indistinguishable from that of the wild-type, PIN2-GFP on the plasma membrane was less polarized in the mutant, and localization on punctate compartments was also evident (Figure 10a,c). Next, I examined the degradative transport of PIN2-GFP to the vacuole. GFP is degraded in the vacuole of *A. thaliana* and not observable under light, but under dark conditions GFP is not degraded

and fluorescence is detectable (Tamura *et al.* 2003), which allows the degradative transport of PIN2-GFP to the vacuole to be monitored (Kleine-Vehn *et al.* 2008). In wild-type plants, accumulation of fluorescence from GFP was observed under dark conditions, reflecting the normal transport of PIN2-GFP to the vacuole. However, in the roots of *vps9a-2* plants, fluorescence was not observed in vacuoles (Figure 10d). Thus, the activity of VPS9a is required for both polar localization and transport of the PIN2 protein to vacuoles.

RAB5 activation is responsible for the expression and localization of PIN3 and PIN4

In the *vps9a-2* mutant, the auxin response maximum shifted towards the root cap. This phenotype reminded me of the phenotype of the triple mutant *pin3 pin4 pin7* (Grieneisen *et al.* 2007). Therefore, I examined whether the *vps9a-2* mutation affects functions of PIN3 and PIN4 by monitoring their expression and intracellular localization in mutant plants. In the wild-type plants, PIN3 expression was detected in tiers two and three of columella cells (Figure 11a) (Blilou *et al.* 2005), whereas PIN3 was detected in tiers one and two in the *vps9a-2* mutant (Figure 11c). For PIN4, expression was confined to tiers one and two of the columella cell layers in wild-type

(Figure 11b) (Friml *et al.* 2002a), and only the first tier of columella cells in *vps9a-2* roots (Figure 11d). Moreover, PIN4 expression was decreased in QC cells and the first tier in the mutant roots (Figure 11d). No clear difference was observed in the polarized localization of PIN3. On the other hand, the polarity of PIN4 in QC cells was compromised in *vps9a-2* roots (Figure 11d). These data indicate that RAB5 activation is required for proper cell-specific expression of PIN3 and PIN4 and the expression level and polarized localization of PIN4 in the columella root cap.

VPS9a is also required for morphogenesis of pavement cells

My findings indicate that auxin-related functions are affected by the *vps9a-2* mutation. Finally, I examined whether aerial parts of the mutant plants also exhibit auxin-related phenotypes. Recently, auxin has been reported to regulate the morphogenesis of leaf pavement cells through ABP1 and ROP GTPase (Sauer and Kleine-Vehn 2011). Therefore, I examined whether the *vps9a-2* mutation also affects the shape of pavement cells. The pavement cells of wild-type leaves exhibited an interlocking jigsaw puzzle-shaped pattern (Figure 12a), but some pavement cells in the mutant plants exhibited a flatter, elongated shape with less interdigitation (Figure 12b). The quantitative analysis (Xu *et al.* 2010) also demonstrated that the number of lobes

per unit in pavement cells in *vps9a-2* was significantly lower than that in wild type (n = 15 cells; P <0.01, Student's *t* test; Figure 12c). This finding suggests that the *vps9a-2* mutation exerted broad effects on root and leaf development, some of which could be attributable to mislocalization of auxin transport and/or signaling molecules.

Discussion

In this study, I demonstrated that proper RAB5 activation is required for RAM activity, cell elongation, and radial patterning in *A. thaliana* roots. I also showed that subcellular trafficking, localization, and/or expression of PIN proteins are affected by the *vps9a-2* mutation. In a consistent manner with the pleiotropic phenotypes, the publicly available database (Brady *et al.* 2007) indicated that *VPS9a* is expressed ubiquitously in the root of *A. thaliana* (figure 13; http://bbc.botany.utoronto.ca/efp/cgi-bin/efpWeb.cgi?dataSource=Root&modeInput=Absolute&primaryGene=AT3G19770). Mutations that affect the auxin response, auxin-dependent gene expression, and localization of auxin transporters have been reported to compromise both cell division and cell expansion in *A. thaliana* roots (Aida *et al.* 2004, Blilou *et al.* 2005, Lincoln *et al.* 1990). Thus, the defects observed in the maintenance of RAM and cell elongation in *vps9a-2* roots might be attributable to aberrant auxin distribution at the QC, columella, and/or stele cells. On the other hand, another plant hormone, gibberellin, is also known to control meristem activity and endodermal cell expansion (Achard *et al.* 2009, Ubeda-Tomas *et al.* 2009). Moreover, gibberellin is reported to be involved in middle cortex formation (Paquette and Benfey 2005). Given that premature middle cortex formation is one of the prominent phenotypes of the *vps9a-2* mutant, RAB5 activation

may also take part in root development through the gibberellin signaling pathway. This notion was further supported by the result that PAC treatment did not enhance the effect of the *vps9a-2* mutation on middle cortex formation. VPS9a is also involved in regulation of the cell number in each cell layer, while the relevance between this phenotype and gibberellin is unclear.

The defective function of RAB5 in endocytic trafficking could also account for the meristematic phenotype observed in *vps9a-2* plants. Recent studies have shown that a well-known LRR receptor-like kinase, CLAVATA1 (CLV1), which plays crucial roles in the maintenance of the shoot apical meristem, is transported from the plasma membrane to the vacuole upon binding a small peptide hormone, CLV3, in a VTI11-dependent manner (Nimchuk *et al.* 2011). This vacuolar traffic is required for CLV3-dependent degradation of CLV1 to attenuate CLV signaling. VTI11 is a Qb-type soluble N-ethylmaleimide-sensitive-factor attachment protein receptor (Qb-SNARE) that mediates membrane fusion with a cognate Qa-SNARE SYP22 in vacuolar transport (Ebine *et al.* 2008, Sanmartin *et al.* 2007). It is also demonstrated that conventional RAB5 and SYP22 cooperatively act in endocytic and vacuolar trafficking pathways (Ebine *et al.* 2011). Considering this with my finding that VPS9a is responsible for the transport of plasma membrane protein PIN2 to the vacuole, my results suggest that

VPS9a is required to modulate peptide hormone signaling via control of the endocytic/vacuolar trafficking pathways, which are responsible for the maintenance of RAM activity.

The *SHR* gene is transcribed in the stele, and translated SHR proteins move from the stele to the endodermis, CEI, and QC cells, where SHR induces the expression of *SCR* (Cui *et al.* 2007, Helariutta *et al.* 2000, Nakajima *et al.* 2001). These processes are essential for the formation and specification of endodermal and cortical cell layers in roots. In mature roots, endodermal cells further divide periclinally to form the middle cortex, which is also dependent on SHR, whereas middle cortex formation is inhibited by SCR (Paquette and Benfey 2005). In *vps9a-2* plants, periclinal division of endodermal cells is observed frequently in young seedlings, whereas such division was rarely observed in wild-type plants at the same developmental stage. The increase in endodermal cell division in young *vps9a-2* roots might be the result of decreased SCR expression in the endodermis, CEI, and/or QC; reduced expression of SCR has been reported to result in extra division of the endodermal cell layer (Cui *et al.* 2007, Welch *et al.* 2007). A mutation in *SCR* has also been reported to cause a decrease in the expression of *SCR* itself in the CEI and QC, which indicates that *SCR* expression in the QC and ground tissue stem cells is auto-regulated (Sabatini *et al.* 2003). Thus, my

results may suggest that efficient activation of RAB5 is required not only for maintaining the expression area of *SHR*, but also for auto-regulatory induction of *SCR* in the QC and CEI cells. Therefore, RAB5 activation seems to be deeply involved in the proper maintenance of the root stem cell niche through two transcription factors, SHR and SCR, which play crucial roles in root development.

Recently, SHR INTERACTING EMBRYONIC LETHAL (SIEL) was isolated as an SHR-interacting molecule and localized on endosomes (Koizumi *et al.* 2011). The function and/or endosomal localization of SIEL may depend on VPS9a function, because VPS9a and RAB5 are essential regulators of endosomal trafficking.

Another remarkable phenotypic abnormality observed in the QC of *vps9a-2* plants is the absence of an auxin response maximum at the QC due to the downward shift of the maximum to the columella cells. This aberrant distribution of auxin could be caused by perturbed distribution, trafficking, and expression patterns of PIN proteins. In *vps9a-2* roots, the localization of PIN2 on the plasma membrane was less polarized. The loss of PIN2 polarity could be due to impaired transport of PIN2 to the vacuole, because proper transport of PIN proteins to the vacuole has been reported to be required for their polar localization (Dhonukshe *et al.* 2008, Jaillais *et al.* 2007, Shirakawa *et al.* 2009, Spitzer *et al.* 2009). In addition to PIN2, PIN3 and PIN4 also play pivotal roles in auxin

distribution in *A. thaliana* roots (Friml *et al.* 2002a, Friml *et al.* 2002b). The expression of PIN4 was decreased and its polar localization in the QC compromised in the mutant roots, whereas the localization of PIN3 was not affected. The decreased expression of PIN4 might be the result of a decreased auxin response at QC cells in mutant roots, because expression of *PIN4* is up-regulated by auxin treatment (Vieten *et al.* 2005). These results could indicate that the subcellular localization of PIN3 is regulated by a different mechanism than PIN2 and PIN4.

Despite the abnormal distribution of auxin, the specification of QC identity did not appear to be affected severely, as all QC markers I examined were expressed properly in *vps9a-2* roots. On the other hand, expression of *SHR* and *SCR* was altered in this mutant; *SHR* is not expressed in the QC of wild-type plants but was frequently expressed in the QC of *vps9a-2* plants, and *SCR* was not detected in the mutant though it is expressed in the QC and CEI of wild-type plants. Because direct indications of auxin-dependent *SHR* and *SCR* expression have not yet been presented, the aberrant distribution of auxin in the *vps9a-2* mutant did not likely cause alterations in the expression patterns of *SHR* and *SCR* directly. My results may indicate that specification of the QC identity is incomplete in the *vps9a-2* mutant because of an absence of the auxin response maximum at the QC (Blilou *et al.* 2005, Sabatini *et al.* 1999), which

indirectly results in aberrant expression of *SHR* and *SCR*.

In addition to the crucial roles of RAB5 activation in root development, I also showed that RAB5 activation is required for the proper development of leaf pavement cells (Figure 12). Thus, the RAB5-dependent trafficking pathway is responsible for various developmental processes in *A. thaliana* at the tissue and organ levels. Future molecular and cellular studies of the regulatory mechanisms of the RAB5-dependent trafficking pathway in combination with analyses of developmental and higher-order functions will uncover the mechanisms underlying the network connecting endosomal trafficking mediated by RAB5 and various plant functions and developmental processes.

Material and Methods

Plant materials and growth conditions

The *A. thaliana vps9a-2* mutant (Columbia accession) was described previously (Goh *et al.* 2007). The transgenic plants expressing reporter proteins were described elsewhere: *cyc1At::GUS* was kindly provided by Gorou Horiguchi (Ferreira *et al.* 1994), *pEn7::YFP*$_{H2B}$ and *pCo2::YFP*$_{H2B}$ were from Renze Heidstra (Heidstra *et al.* 2004), *pSHR::GFP* and *pSCR::GFP* were gifts from Philip Benfey (Helariutta *et al.* 2000, Wysocka-Diller *et al.* 2000), *pWOX5::GFP* was from Thomas Laux (Sarkar *et al.* 2007), *QC46::GUS* and *QC184::GUS* were from Ben Scheres (Sabatini *et al.* 1999), *pDR5::GFP* was from Jiri Friml (Friml *et al.* 2003), and *pVND3::YFP-nuc* was provided by Masatoshi Yamaguchi and Taku Demura (Kubo *et al.* 2005). The Columbia (Col) accession was used as the wild-type. The *vps9a-2* mutant plants were crossed with *cyc1At::GUS*, *pEn7::YFP*$_{H2B}$, *pCo2::YFP*$_{H2B}$, *pSHR::GFP*, *pSCR::GFP*, *pWOX5::GFP*, *QC46::GUS*, *QC184::GUS*, or *pDR5::GFP* reporter lines, and F2 plants with the homozygous *vps9a-2* mutation and homozygous or heterozygous reporter gene were used for analyses.

Seeds were sterilized in 1% sodium hypochlorite and 0.1% Triton X-100, rinsed with sterile distilled water three times, and sown on Murashige & Skoog medium

(pH 6.3) supplemented with 2% sucrose, 0.3% Gellan gum, and 1×Gamborg's vitamins. The plants were incubated for 2 days at 4°C in the dark, and cultivated at 23°C under continuous light.

GUS staining

Seedlings were incubated in acetone at -20°C and then incubated in staining solution (100 mM sodium phosphate buffer pH 7.0, 10 mM EDTA, 0.5 mM potassium ferricyanide, 0.5 mM potassium ferrocyanide, 0.1% Triton X-100, and 0.5 mg/ml X-glucuronide) at 37°C for 1 or 2 hr. Samples were washed with distilled water and then mounted in a clearing solution (8 g chloral hydrate in 1 ml glycerol and 2 ml water) on glass microscope slides.

PI staining

Root tips were stained with 20 mg/ml propidium iodide (PI) solution and observed using a LSM710 confocal laser-scanning microscope (Carl Zeiss).

Paclobutrazol treatment

For PAC treatment, wild-type and *vps9a-2* mutant plants were sown and grown

on MS plantes containing 0 nM or 5 nM paclobutrazol (purchased from Wako Pure Chemical Industries).

.

Immunostaining

Whole-mount immunolocalization of PIN proteins was performed using roots from 5 to 7-day-old seedlings as described previously (Friml *et al.* 2002a, Friml *et al.* 2002b, Muller *et al.* 1998, Paciorek *et al.* 2005) and observed under a LSM710 confocal laser-scanning microscope (Carl Zeiss).

Microscopic Observation of Leaf pavement cells

The third true leaves from 2-week-old seedlings were incubated in a clearing solution (8 g chloral hydrate in 1 ml glycerol and 2 ml water) until the tissues became transparent. The abaxial side of the leaves was observed under a light microscope (BX60; Olympus) equipped with a CCD camera (DP73; Olympus).

Accession Numbers

The Arabidopsis Genome Initiative locus identifiers for the genes mentioned in this article are At3g19770 (*VPS9a*), At5g45130 (*ARA7*), At5g45130 (*RHA1*),

At3g54840 (*ARA6*), At4g27490 (*cyc1At*), At4g28100 (*En7*), At1g62500 (*Co2*), At4g37650 (*SHR*), At3g54220 (*SCR*), At3g11250 (*WOX5*), At5g66300 (*VND3*), Atg57090 (*PIN2*), At1g70940 (*PIN3*) and At2g01420 (*PIN4*).

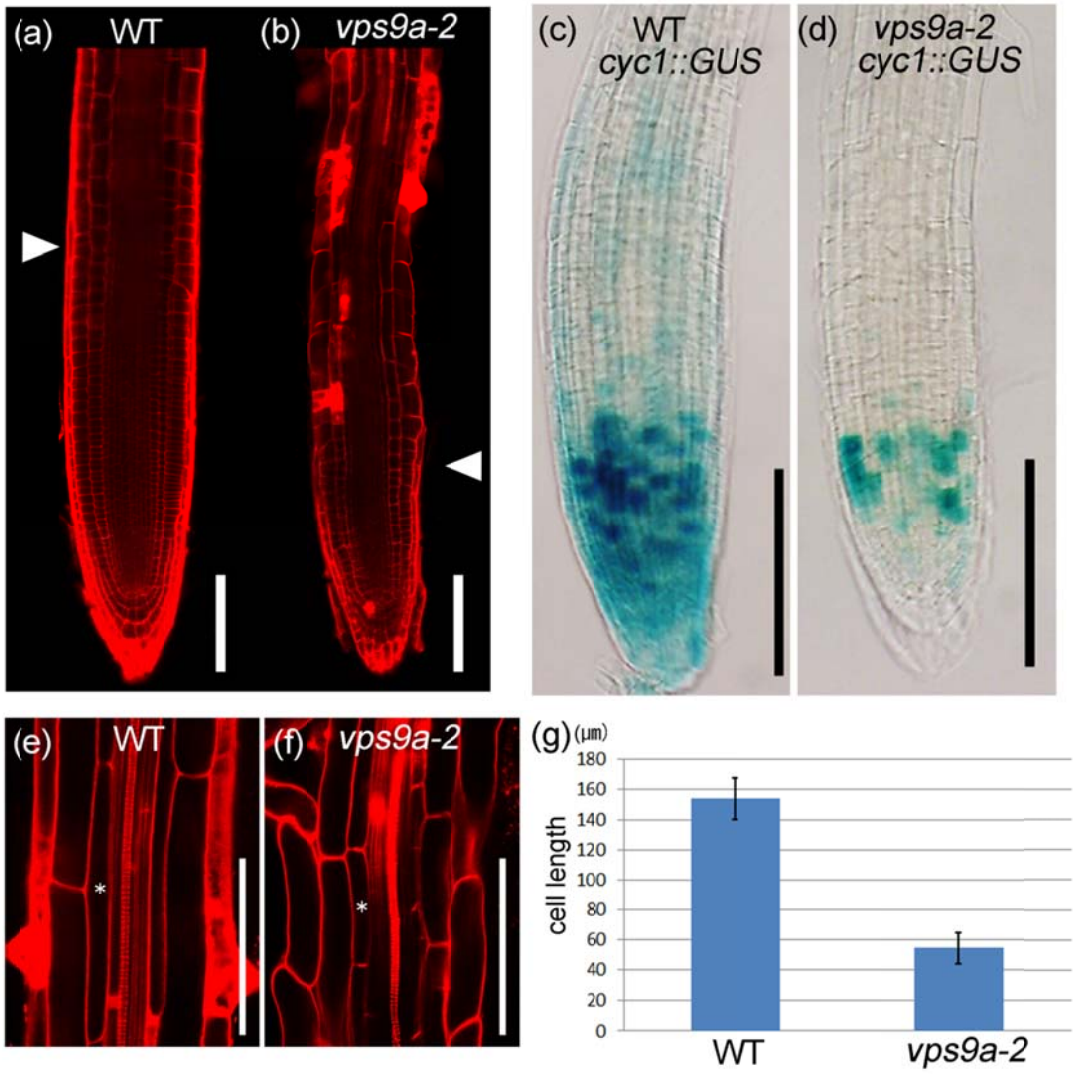

Figure 1. The *vps9a-2* roots were defective in both cell division and cell elongation. (a,b) Size of the root apical meristem of wild-type (WT) and *vps9a-2* plants. Arrowheads indicate the boundary between the division and elongation zones. Scale bar = 100 μm. (c,d) Mitotic activities in WT and *vps9a-2* roots were monitored by the *cyc1At::GUS* reporter. Scale bar = 150 μm. (e,f) Endodermal cells (asterisks) at the boundary between the elongation and differentiation zones of WT and *vps9a-2* roots. Scale bar = 100 μm. (g) Length of the endodermal cells around the boundary between the elongation and differentiation zones of WT (154±14 μm) and *vps9a-2* (55±11 μm) roots. Results are given as means ± S.D.

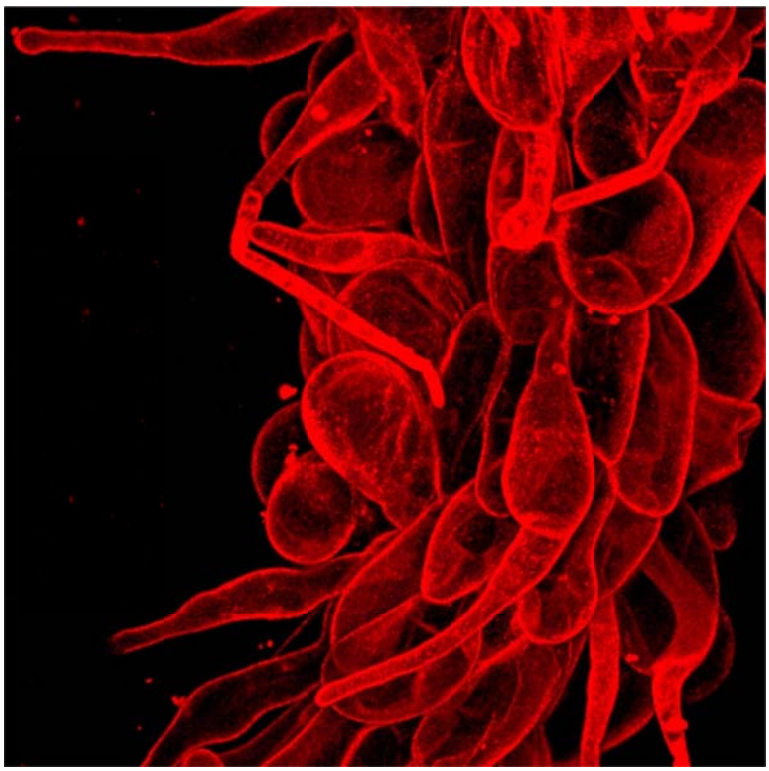

Figure 2. 3D projection constructed from Z-stack images of a 5-day-old *vps9a-2* root stained with propidium iodide. The epidermal cells of the mutant root swelled and exfoliated.

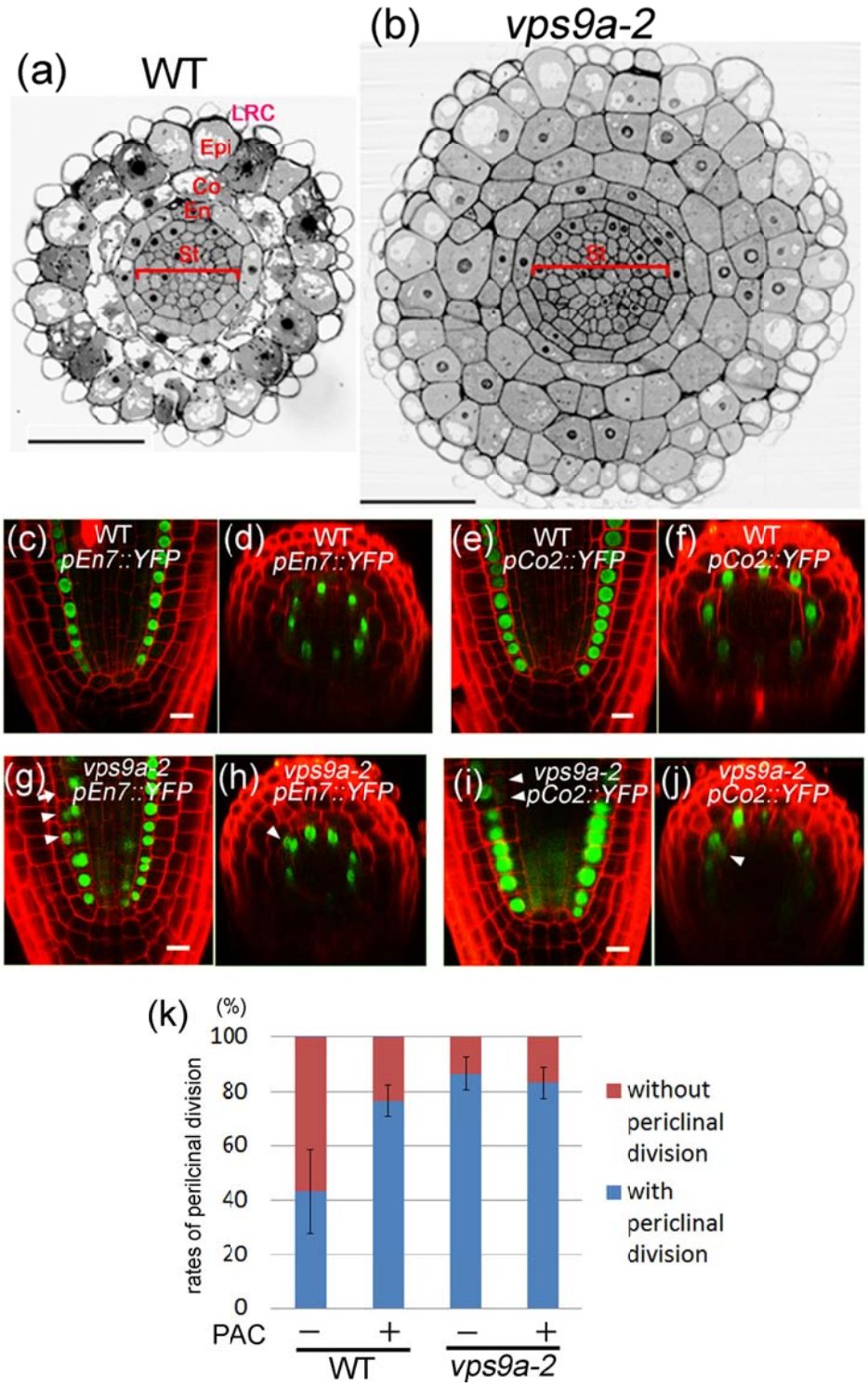

Figure 3. The *vps9a-2* roots form middle-cortex more frequently than wild-type (WT) roots and are defective in the ground tissue patterning. (a,b) Transverse sections of WT and *vps9a-2* roots. The number of epidermal, cortical, and endodermal layers was four to six in *vps9a-2*, whereas that of WT was three (one of each layer). The number of cells

in each cell layer of the *vps9a-2* mutant was also larger than that of wild-type. Brackets indicate the stele. St, stele; En, endodermis; Co, cortex; Epi, epidermis; and LRC, lateral root cap. (c-f) Confocal images showing the expression pattern of *pEn7::YFP*$_{H2B}$ (c,d) and *pCo2::YFP*$_{H2B}$ (e,f) in WT roots. (g-j) Confocal images showing the expression pattern of *pEn7::YFP*$_{H2B}$ (g,h) and *pCo2::YFP*$_{H2B}$ (i,j) in *vps9a-2* roots. Some of the outer daughter cells in (g) and (h) retained their endodermal identity after periclinal division (arrowheads), whereas others lost the identity (arrow). The outer daughter cells in (i) and (j) that acquired a cortical identity are indicated by arrowheads. Scale bar = 10 μm. (k) Frequency of middle cortex formation in untreated WT (43±15%), WT treated with 5 nM paclobutrazol (PAC, 77±6%), untreated *vps9a-2* (87±6%), and *vps9a-2* treated with 5 nM PAC (84±6%) roots 3 DAG. The results are provided as means ± SD.

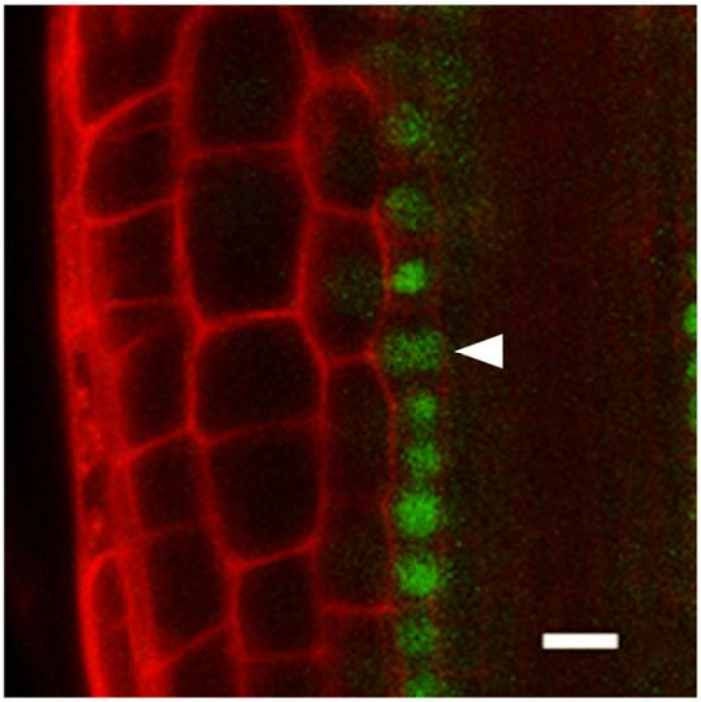

Figure 4. Inner daughter cell (arrowhead) of endodermis that divided periclinally after periclinal division in the mutant root. Scale bars = 10 μm.

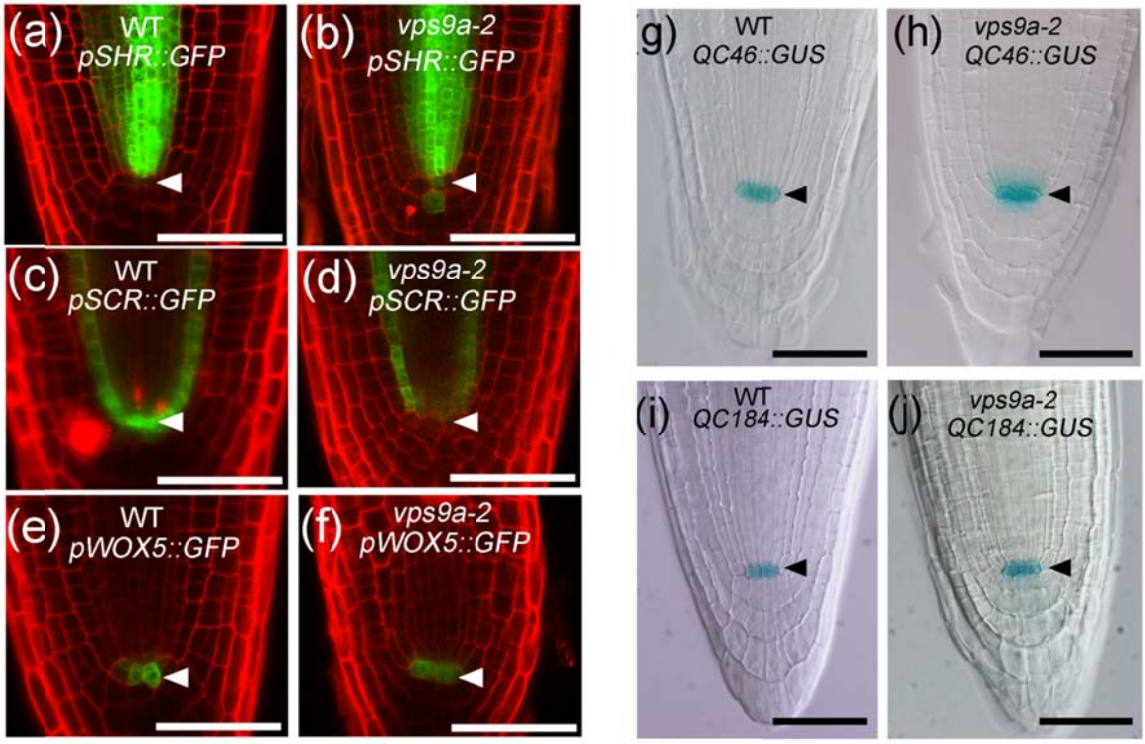

Figure 5. The *vps9a-2* roots exhibit defects in the localization of *SHR* and *SCR* expression within the stem cell niche. (a,b) Confocal images showing the expression pattern of *pSHR::GFP* in wild-type (WT) and *vps9a-2* roots, (c,d) *pSCR::GFP* in WT and *vps9a-2* roots, and (e,f) *pWOX5::GFP* in WT and *vps9a-2* roots. (g-j) Expression of QC identity markers, QC46::GUS (g,h) and QC184::GUS (i,j), in WT and *vps9a-2* roots. Arrowheads indicate QC cells. Scale bar = 10 μm.

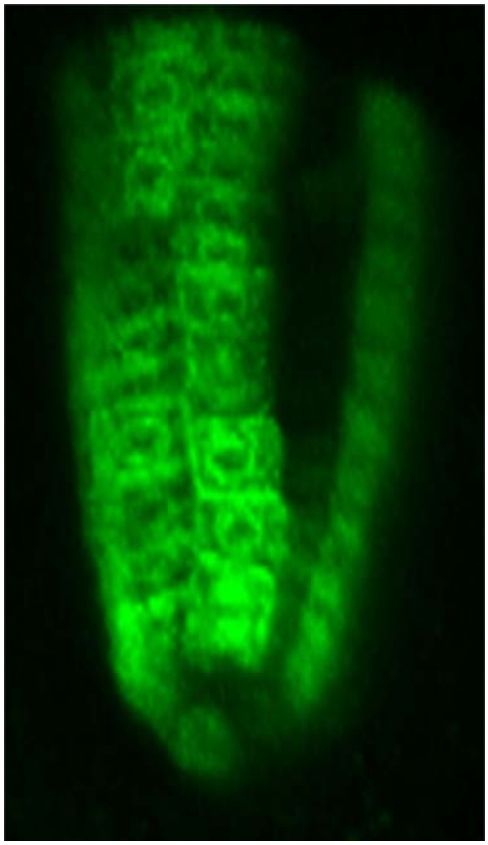

Figure 6. Expression of SCR decreased in the QC and endodermal cells of *vps9a-2* roots. The side view of the expression pattern of *pSCR::GFP* in *vps9a-2* roots is indicated (projection of confocal Z-stack images).

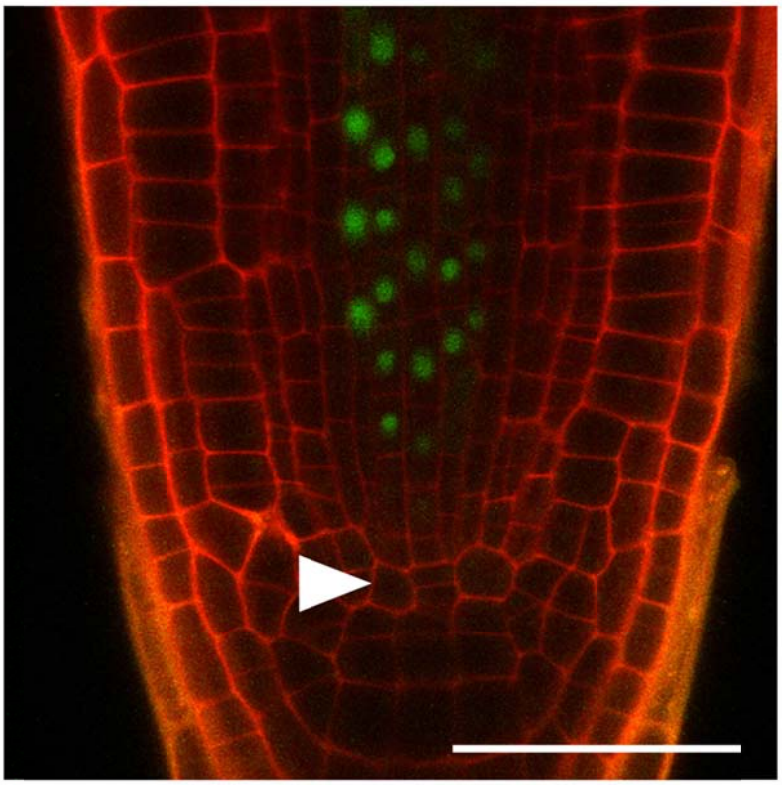

Figure 7. QC cells in *vps9a-2* roots did not harbor the procambial identity. Expression of pVND3::YFP-nuc, a procambial marker, was not detected in the QC cells of *vps9a-2* roots.

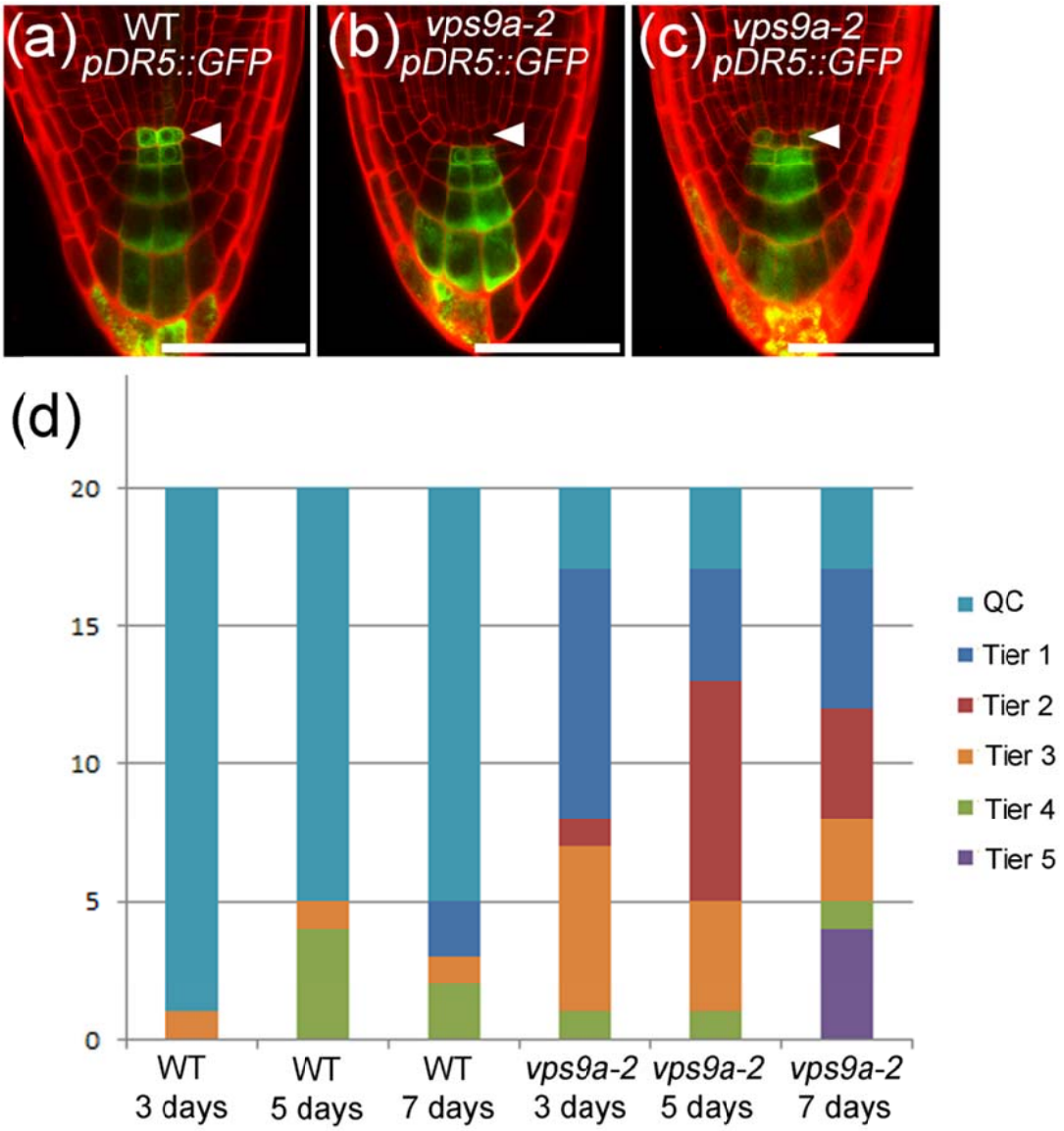

Figure 8. The *vps9a-2* roots are defective in the positioning of auxin maxima in the root tips. (a-c) Confocal images showing the expression pattern of *pDR5::GFP* in wild-type (WT) and *vps9a-2* roots. Arrowheads indicate the QC cells. Scale bar = 50 μm. (d) Position of the auxin response maxima in WT and *vps9a-2* roots. Most WT roots establish an auxin response maxima at the QC cells (light blue bars), whereas the auxin response maxima in *vps9a-2* roots shift toward the root tips.

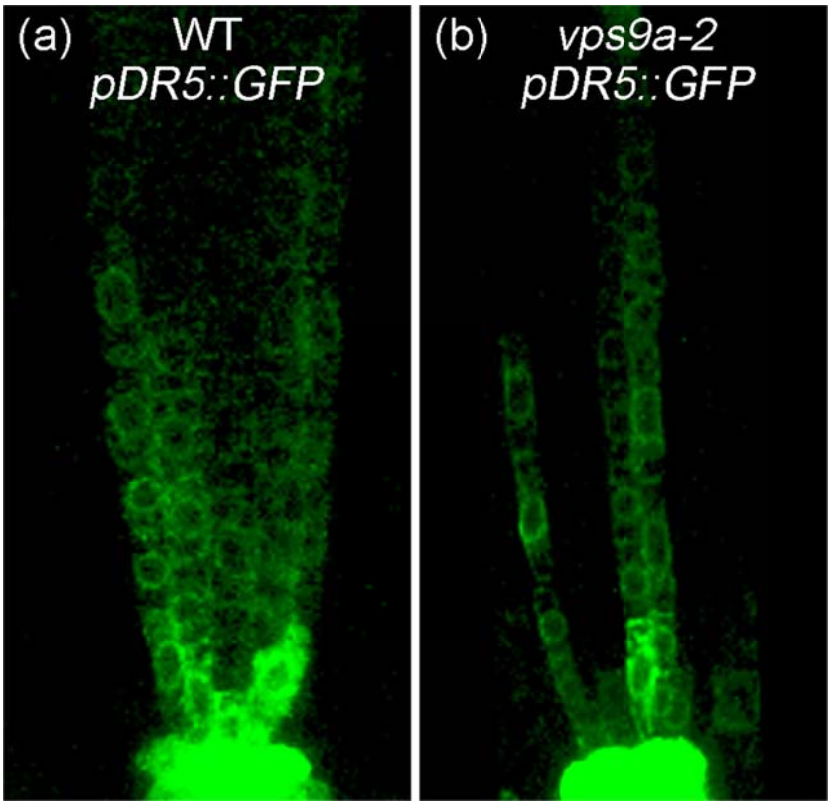

Figure 9. Expression patterns of auxin-responsive reporter pDR5::GFP were different between roots from *vps9a-2* and wild-type plants. (a) pDR5::GFP expression was observed in a sheet-like pattern, including metaxylem and protoxylem in the stele of wild-type roots, (b) whereas the expression area was decreased in *vps9a-2* roots.

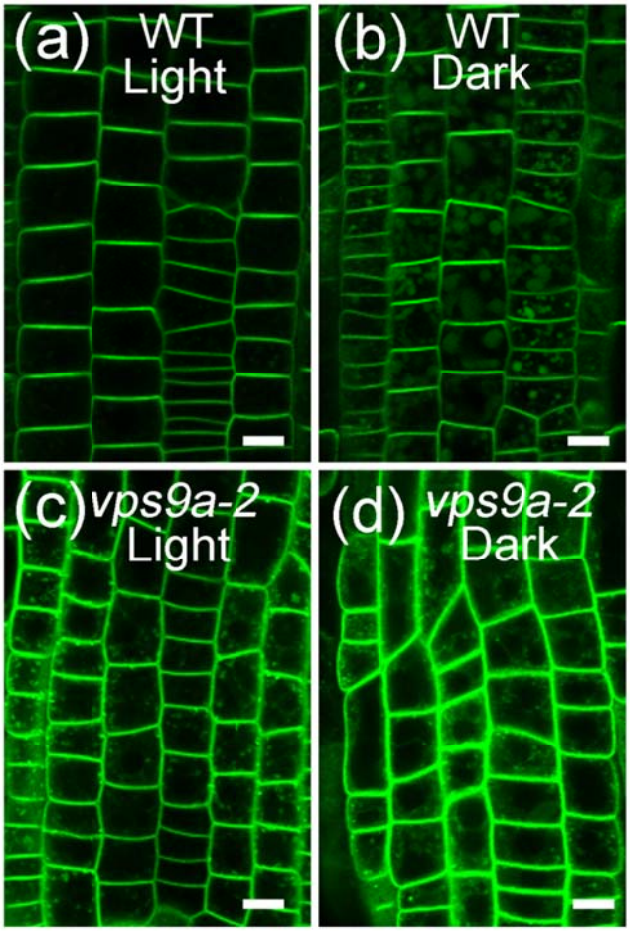

Figure 10. Defective PIN2 transport into vacuoles in the *vps9a-2* mutant. (a,b) Expression pattern of PIN2-GFP in wild-type (WT) roots under continuous light (a) and dark (b) conditions. (c,d) Expression pattern of PIN2-GFP in *vps9a-2* roots under continuous light (c) and dark (d) conditions. Scale bar = 10 μm.

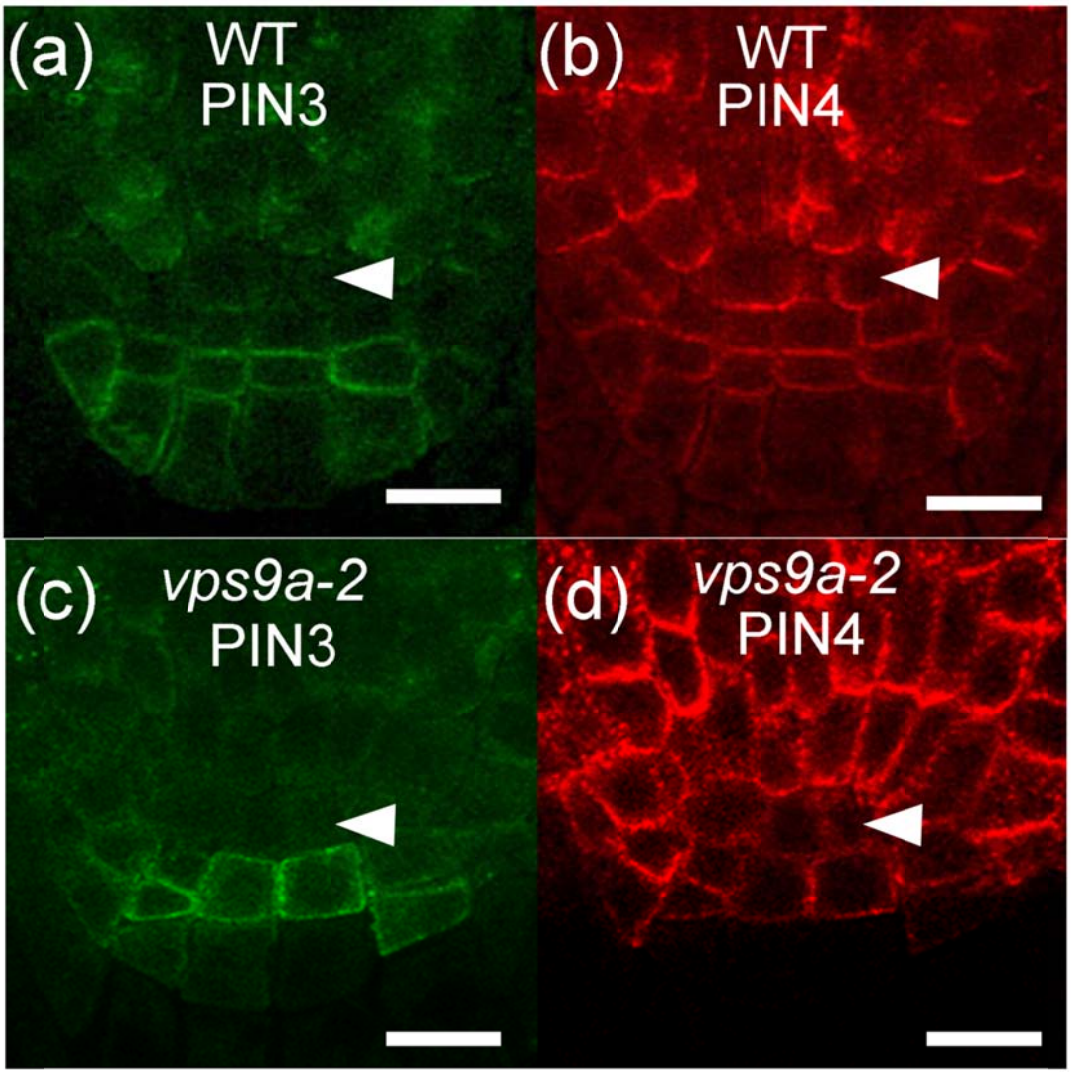

Figure 11. Sites of PIN3 and PIN4 expression shift downward in *vps9a-2* roots. Immunostaining of PIN3 (a,c) and PIN4 (b,d) in the root caps of wild-type (WT) (a,b) and *vps9a-2* (c,d) plants. 5-day-old seedlings were immunostained. Arrowheads indicate QC cells. Scale bar = 10 μm.

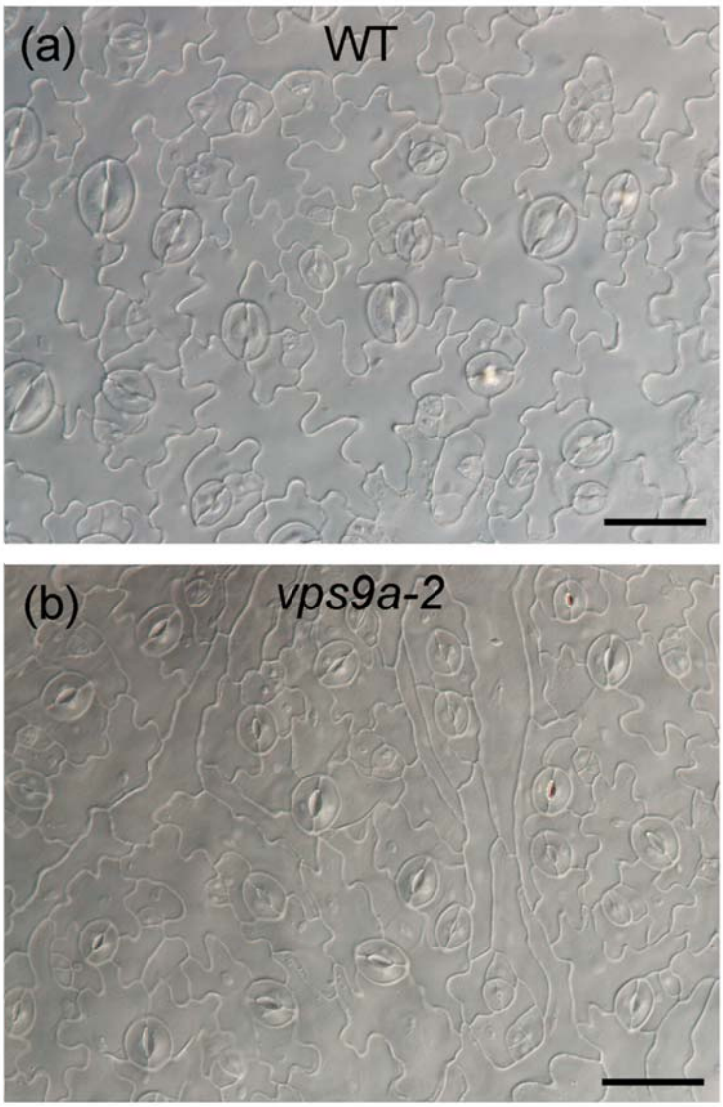

Figure 12. The *vps9a-2* mutant exhibits a defect in pavement cell shape. (a) The pavement cells of wild-type (WT) leaves have an interlocking jigsaw puzzle-shaped pattern. (b) The *vps9a-2* mutant displays loss of the interdigitation. Scale bar = 50 μm. (c) Quantification of the lobe number per unit in pavement cells in leaves of wild-type (WT) and *vps9a-2* plants.

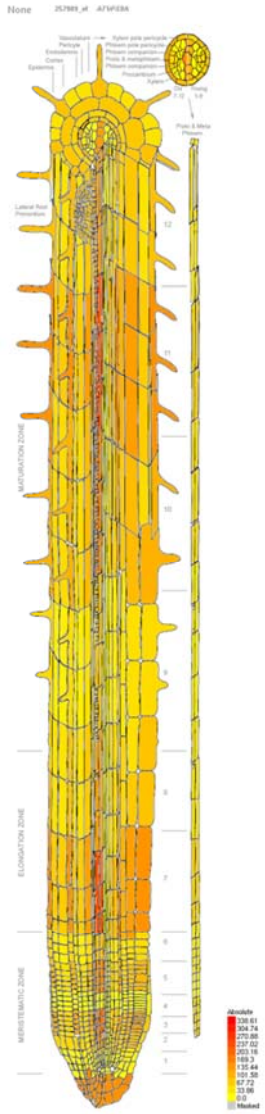

Figure 13
VPS9a is ubiquitously expressed in the roots according to high-resolutionspatiotemporal gene expression map (http://bbc.botany.utoronto.ca/efp/cgi-bin/efpWeb.cgi?dataSource=Root&modelnput=Absolute&primaryGene=AT3G19770).

Chapter 2

Plant vacuolar trafficking occurs through distinctly regulated pathways

Introduction

Plant cell vacuoles contain lytic compartments similar to those of animal lysosomes and yeast vacuoles. They also fulfil diverse unique functions including the storage of proteins and sugars, maintenance of turgor, and increase of cell volume. The structure and function of the vacuole dynamically change in response to extracellular and intracellular conditions (Gao *et al.* 2005, Hamaji *et al.* 2009, Hatsugai *et al.* 2009, Saito *et al.* 2005). Embryonic cells contain large protein storage vacuoles (PSVs), which rapidly acquire the identity of the lytic vacuole during seed germination (Bolte *et al.* 2011, Marty 1999). The dynamic and highly organised functions of plant vacuoles are fulfilled through tight regulation of trafficking to and from the vacuoles, which involves evolutionarily conserved machinery components such as RAB GTPases. RAB GTPase is a central regulator of membrane traffic that regulates tethering and fusion between trafficking carriers and target membranes (Barr 2013). Although the basic framework of the RAB GTPase action is well conserved in eukaryotic cells (Ackers *et al.* 2005, Kremer *et al.* 2013, Mizuno-Yamasaki *et al.* 2012, Nakada-Tsukui *et al.* 2010, Niihama *et al.* 2009, Saito and Ueda 2009), recent comparative genomic studies suggest that each eukaryotic lineage has acquired a unique repertoire of RAB GTPases during evolution (Dacks and Field 2007, Dacks *et al.* 2008, Mackiewicz and Wyroba 2009). Plants also

harbour a unique set of RAB GTPases partly characterised by functional diversification of the RAB5 group acting in endosomal/vacuolar trafficking pathways (Ebine *et al.* 2012). RAB7 is also proposed to regulate vacuolar traffic in plants (Pedrazzini *et al.* 2013). In animal cells, RAB5 and RAB7 act in a sequential manner mediated by the effector complex HOPS (Rink *et al.* 2005) and a guanine nucleotide exchange factor (GEF) for RAB7 consisting of SAND1/Mon1 and CCZ1 (Bohdanowicz and Grinstein 2010). The sequential interaction of these components is responsible for the maturation from early to late endosomal compartments (Kinchen and Ravichandran 2010, Poteryaev *et al.* 2010). Conversely, how the vacuolar trafficking pathway is organised by RAB5 and RAB7 in plant cells remains mostly unknown. To examine the regulatory mechanism of vacuolar transport by RAB5 and RAB7 in *Arabidopsis thaliana*, I examined the defects in vacuolar trafficking in the *vps9-2* mutant, a weak mutant allele of RAB5 GEF, and the mutant of CCZ1, which forms a complex with SAND1 and serves as the GEF for RAB7. Comparing transport of soluble and membrane cargos to the vacuole between these mutants, I found that the plant harbors not only the conserved vacuolar trafficking pathway regulated by the sequential action of RAB5 and RAB7, but also a unique route regulated by RAB5 without RAB7.

Results

SAND1 and CCZ1a/b form a complex and act as the GEF for RAB7 in *Arabidopsis thaliana*

To elucidate the contribution of RAB5 and RAB7 (also called RABF and RABG in *A. thaliana*, respectively) in the targeting and biogenesis of vacuoles, I first characterised the *A. thaliana* homologs of *SAND1* and *CCZ1*, the key mediators of endosomal maturation in animal and yeast cells, which form a complex and act as the GEF of the RAB7 group in animal and yeast cells. The *A. thaliana* genome contains one *SAND1* homolog and two *CCZ1* homologs (*CCZ1a* and *CCZ1b*). I tested interactions between the products of these genes by three methods. The yeast two-hybrid analysis revealed that both CCZ1a and CCZ1b interacted with SAND1 in yeast cells (Figure 14a). This interaction was confirmed by co-immunoprecipitation from the lysate of transgenic plants expressing GFP-tagged CCZ1a protein (Figure 14b). SAND1 coimmunoprecipitated with GFP-CCZ1a but not with GFP. This complex formation was also ascertained by co-purification of these proteins from lysates of *E. coli* expressing GST-SAND1 and hexahistidine (His_6)-tagged CCZ1b using glutathione sepharose (Figure 14c).

Next, I attempted to detect nucleotide exchange in RAB7 mediated by the purified SAND1-CCZ1 complex and found that soluble RAB7 was not activated by this complex. For a more efficient interaction between the RAB protein and the SAND1-CCZ1 complex, I constructed C-terminally His_6-tagged RAB7/RABG3f and immobilised it on liposomes containing DOGS-NTA lipids (1,2-dioleoyl-sn-glycero-3-[(N-(5-amino-1-carboxypentyl)iminodiacetic acid)succinyl]), which was expected to mimic the interaction between RAB7 and the membrane and was successfully used for detecting the GEF activity toward the yeast RAB7 homolog Ypt7p (Cabrera *et al.* 2014). This strategy allowed me to detect specific and concentration-dependent GEF activity of SAND1-CCZ1a for plant RAB7 (Figure 15), thus demonstrating that the function of the SAND1-CCZ1 complex is conserved between plants and other kingdoms.

SAND1/CCZ1 complex is colocalized with RAB5 and RAB7 on endosomes

To understand the function of the SAND1/CCZ1 complex, I established the mutant lines of those genes. The loss of function of *SAND1* resulted in a severe growth defect, and the double mutant *ccz1a ccz1b* exhibited a slightly weaker growth defect than the *sand1* mutant (Figure 16a and b). However, single *ccz1* mutants were

indistinguishable from the wild-type plant (Figure 16c), which means that CCZ1a and CCZ1b share at least partially redundant functions. Fluorescently tagged SAND1, CCZ1a, and CCZ1b, all of which rescued the growth defects found for the respective mutants (Figure 17). This result indicated that the growth defects of the mutants are due to the mutation of respective genes and fluorescently tagged proteins are functional.

Fluorescently tagged SAND1, CCZ1a, and CCZ1b colocalized to punctate compartments that were stained by the endocytic tracer FM4-64 (Figure 18a), indicating their endosomal localization. Some of the SAND1- or CCZ1-positive compartments also colocalized with the RAB7 member RABG3f, which is consistent with a function as a GEF for RAB7 (Figure 18b). Intriguingly, better colocalization with CCZ1a was observed for the RAB5 members ARA7/RABF2b and ARA6/RABF1 (Figure 18b). This result could reflect recruitment of the SAND1/CCZ1 complex by active GTP-bound RAB5 to the endosome as previously reported in an animal system. The Golgi marker ST-mRFP and the *trans*-Golgi network (TGN) marker VHA-a1-mRFP localized to distinct compartments from SAND1/CCZ1, whereas VHA-a1-mRFP was occasionally observed to associate with SAND1/CCZ1 compartments (Figure 18c). These results supported the function of the SAND1-CCZ1 complex as the GEF of RAB7.

CCZ1 is required for vacuolar membrane localization of RAB7

To elucidate the effects of mutations in *SAND1* and *CCZ1* on the distribution of RAB7 and RAB5, I then evaluated the localization of RABG3f and RAB5 family members in the relevant mutants. RABG3f was mainly localized to the vacuolar membrane in wild-type plants, although some of which was also found on punctate endosomes (Figure 19). In *ccz1a ccz1b*, RABG3f failed to localize to the vacuolar membrane but was found in the cytosol in addition to punctate compartments that were not stained by FM4-64, although these compartments were frequently associated with FM-stained compartments (Figure 19). This result demonstrated that CCZ1 is required for the proper localization of RAB7 and suggested that RAB7 localize to the vacuolar membrane when activated by the SAND1/CCZ1 complex.

Seed storage proteins are transported to the vacuole via the RAB5- and RAB7-dependent pathway

I then examined the localization of RAB5 family members (RHA1 and ARA6) in wild-type and the *ccz1a ccz1b* mutant plants. While both RHA1 and ARA6 localized to punctuate compartments in wild-type plants (Figure 20a), RAB5-positive compartments with dilated ring-shaped structures clustered in the cytoplasm and were stained by

FM4-64, indicating that these structures retain endosomal properties (Figure 20b). Given that RAB5 localizes to small punctate endosomes in wild-type plants, the dilated morphology of the RAB5-positive compartments suggested that transport and/or maturation from RAB5-positive endosomes to the next destination, likely the late endosome or vacuole, was impaired in mutant plants. These lines of evidence strongly support the existence of endosomal trafficking/maturation from RAB5- to RAB7-positive endosomes through sequential action of RAB5 and RAB7, as previously proposed in both animal and plant cells (Bohdanowicz and Grinstein 2010, Bottanelli *et al.* 2012, Limpens *et al.* 2009, Rink *et al.* 2005). I also noted that endocytic transport of FM4-64 to the vacuolar membrane was not remarkably impaired in *ccz1a ccz1b* (Figure 21), which suggests the existence of a RAB7-independent vacuolar trafficking pathway in *A. thaliana*.

I next investigated vacuolar transport in embryos. I examined and compared the processing of 12S globulin in wild-type, *ccz1a ccz1b,* and *vps9a-2* (an allele of a RAB5 GEF mutant) seeds to monitor the defect in trafficking to the PSVs, and I found that precursors of 12S globulin accumulated in the *ccz1a ccz1b* and *vps9a-2* mutants while no precursor was detected in the wild type (Figure 22a). This result indicates that both RAB5 and RAB7 are required for maturation of seed storage proteins. Next I observed

mature seeds with *ccz1a ccz1b* and *vps9a-2* expressing GFP-CT24 (Fuji *et al.* 2007, Nishizawa *et al.* 2003) and found that GFP-CT24 was mis-secreted to the extracellular space in both *ccz1a ccz1b* and *vps9a-2* (Figure 22b). Intriguingly, the morphology of the PSV exhibited distinct sensitivity to these mutations. The PSVs in *ccz1a ccz1b* mutants exhibited severe fragmented (or unfused) morphology, whereas the *vps9a-2* mutation did not affect PSV morphology. Immuno-EM further demonstrated that 12S globulin was also mis-secreted to the extracellular space in these mutants. This common phenotype is consistent with the notion that these proteins are transported via the trafficking pathway regulated by the sequential action of RAB5 and RAB7. However, in addition to the typical extracellular accumulation of mis-secreted proteins as observed in *vps9a-2*, large aggregating structures with GFP-CT24 fluorescence were also observed in *ccz1a ccz1b*. EM observation indicated that these structures were large paramural bodies with numerous exosome-like vesicles (Figure 22c). I did not observe such structures in *vps9a-2* seeds. This difference in phenotype again suggests that RAB7 and RAB5 have at least partially distinct functions.

SYP22 is transported to the vacuolar membrane by a unique pathway

Next, I asked how RAB5 and RAB7 function in the trafficking of membrane

proteins. I expressed two vacuolar membrane proteins, mRFP-SYP22 and/or GFP-VAMP713, in mutants defective in the RAB5- (*vps9a-2*) or RAB7- (*ccz1a ccz1b*) dependent trafficking pathway and examined their localization in root epidermal cells (Figure 23, 24). GFP-VAMP713 was not markedly affected by *vps9a-2*, indicating that activation of RAB5 is not critical for targeting of VAMP713 to the vacuole. The *ccz1a ccz1b* mutation did not substantially alter the localization of VAMP713, which suggests that RAB7 also could be dispensable for transport of this protein to the vacuole. Thus, the trafficking pathway responsible for the vacuolar localization of VAMP713 depends on neither RAB7 nor RAB5. On the other hand, the majority of mRFP-SYP22 was mis-targeted to the plasma membrane and punctate compartments in the cytoplasm in *vps9a-2*. The vacuolar localization of mRFP-SYP22 was insensitive to the *ccz1* mutations, whereas fragmentation of the vacuole was evident in these mutants. Thus, transport of mRFP-SYP22 to the vacuole requires RAB5 activation, but active RAB7 seems to be dispensable for transport of SYP22 to the vacuole.

Discussion

As shown above, analyses of the SAND1/CCZ1 complex indicated that plant cells are also equipped with a vacuolar trafficking pathway in which the SAND1/CCZ1 complex mediates the sequential action of RAB5 and RAB7 and leads to endosomal maturation. This trafficking pathway contributes to the transport of storage proteins to PSVs, which is supported by the finding that *ccz1a ccz1b*, and *vps9a-2* mutants share the common phenotype of mis-secreting storage proteins. Conversely, evaluation of RAB7- and RAB5-related mutants demonstrated that multiple trafficking pathways that do not require the sequential action of RAB5 and RAB7 also operate in plant vacuolar trafficking (Figure 25). The unique property of the trafficking pathway of mRFP-SYP22 should be especially emphasised; it requires RAB5 but not RAB7, and such a pathway has never been reported in an animal system. The transport route of GFP-VAMP713 also offers interesting insight into vacuolar transport in plants. This trafficking pathway seems to require activation of neither RAB5 nor RAB7. This result suggests that in addition to the route commonly used by endocytic and vacuolar trafficking pathways, plant cells could have another vacuolar trafficking pathway independent of the endocytic pathway for which endocytic RAB GTPases such as RAB5 and RAB7 are not required. Another unknown RAB GTPase could be responsible for transport of

VAMP713 to the vacuole. RAB11 is a candidate molecule for such activity, as its diverse roles in post-Golgi trafficking have been recently suggested (Choi *et al.* 2013). Alternatively, my result may indicate that the functions of RAB5 and RAB7 are interchangeable and that either of them is sufficient for vacuolar targeting of VAMP713. However, this possibility is not likely given the tightly regulated specificity of RAB function in the membrane trafficking system. SYP22 has been proposed to be transported to the vacuole in a RAB7-dependent and RAB5-independent manner in tobacco (Bottanelli *et al.* 2011), whereas my results indicate that SYP22 does not require RAB7 to reach the vacuole in *A. thaliana*. The reason for this apparent discrepancy is not clear, but it could reflect distinct trafficking systems employed in different plant species or tissues or the distinct experimental systems employed in these studies.

As shown above, plants have developed a unique vacuolar trafficking system by recruiting conserved molecular machinery to trafficking pathways distinct from those in non-plant systems, and also by adding original molecular machinery such as VAMP727 into this system (Ebine *et al.* 2008). My results indicate that each trafficking route is responsible for the transport of particular cargos, suggesting that the mechanism of cargo sorting should be investigated in parallel with studies on docking and fusion

machinery involving RAB GTPases. Further studies to unravel the mechanisms of cargo sorting at donor organelles including the ER, Golgi, and TGN in addition to detailed analyses on docking and fusion mechanisms at the target vacuolar membrane will help to construct a whole image of the vacuolar transport system in plants that was acquired to play fundamental roles in various plant functions. These studies will also shed light on how eukaryotic cells have expanded membrane trafficking pathways in a lineage-specific manner and how the newly pioneered trafficking pathways were recruited to fulfil novel and specialised organelle functions such as vacuole functions in the land plant lineage.

Material and Methods

Plant Materials and growth conditions

A. thaliana *sand1-1* (SALK_075382), *ccz1a* (SALK_048984), *ccz1b* (SAIL_70D10) mutants were obtained from ABRC (Alonso *et al.* 2003), and *sand1-2* (GABI_397H04) was obtained from GABI–KAT (Rosso *et al.* 2003). The mutants were backcrossed at least three times to wild-type *A. thaliana* (Columbia). *vps9a-2* was obtained from lab stocks (Ebine *et al.* 2011, Goh *et al.* 2007). The construction of ARA6-XFP, Venus-RHA1, mRFP-ARA7, GFP-VAMP713, and mRFP-SYP22 expressed under the native promoters was described previously (Ebine *et al.* 2011, Ebine *et al.* 2008). Translational fusions between the cDNA for fluorescent proteins and *A. thaliana* genes were generated using the In-Fusion cloning kit (Clontech). cDNA encoding GFP or mRFP was inserted in front of the start or stop codon of each gene as follows: *SAND1* (At2g28390), 2.1 kb of the 5'-flanking sequence and 1.4 kb of the 3'-flanking sequence; *CCZ1a* (At1g16020), 1.5 kb of the 5'-flanking sequence and 1.0 kb of the 3'-flanking sequence; and *CCZ1b* (At1g80910), 1.3 kb of the 5'-flanking sequence and 1.3 kb of the 3'-flanking sequence. The chimeric genes were then subcloned into pGWB1, pBGW, or pHGW. The plasmid containing SP-GFP-CT24 and transgenic plants expressing SP-GFP-CT24 were kindly provided by S. Utsumi.

Transformation of *A. thaliana* plants was performed by floral dipping using *Agrobacterium tumefaciens* (strain GV3101::pMP90).

Seeds were sterilized in 1% sodium hypochlorite and 0.1% Triton X-100, rinsed with sterile distilled water three times, and sown on Murashige & Skoog medium (pH 6.3) supplemented with 2% sucrose, 0.3% Gellan gum, and 1×Gamborg's vitamins. The plants were incubated for 2 days at 4°C in the dark, and cultivated at 23°C under continuous light.

Light Microscopy

For imaging of protein storage vacuoles, the samples were excited with the laser and autofluorescence was observed. Observations were conducted using LSM710 or LSM780 (Carl Zeiss). For labelling with FM4-64 (Invitrogen), the samples were incubated in MS cell culture medium (Sigma-Aldrich Co.) supplemented with 4 μM FM4-64 for 30, 45 or 60 min at 23 °C and then observed.

Antibodies

Glutathione S-transferase **(**GST)-tagged N-terminal regions of SAND1 (199 amino acids), CCZ1a (165 amino acids), and CCZ1b (167 amino acids) were expressed

in the *E. coli* BL21 strain using the pGEX4T-1 vector (GE Healthcare) and bound to glutathione-Sepharose 4B (GE Healthcare). Column matrix-bound GST-fused proteins were then cleaved with thrombin, and the N-terminal regions of SAND1, CCZ1a, and CCZ1b were eluted and concentrated using Amicon Ultra-15 centrifugal filters (Millipore). The purified proteins were used as antigens to raise polyclonal antibodies in rabbits. For affinity-purification of the anti-CCZ1b antibody, maltose-binding protein (MBP)-tagged CCZ1b (497 amino acids) was also expressed in the *E. coli* Rosetta strain using the pMAL-c2X vector (New England Biolabs). MBP-CCZ1b was purified using amylose resin (New England Biolabs) according to the manufacturer's instructions. The anti-CCZ1b antibody was purified using the HiTrap protein G HP Column (GE Healthcare) and then affinity-purified using the MBP-CCZ1b-coupled HiTrap NHS-activated HP column (GE Healthcare) according to the manufacturer's instructions. The elution buffer was changed to PBS, and the protein was concentrated using Amicon Ultra-15 centrifugal filters (Millipore).

The antibodies were used for immunoblotting at 1:500 for the anti-GST, anti-SAND1, anti-CCZ1b, and anti-GFP antibodies; at 1:100 for the affinity-purified anti-SAND1 antibody; and at 1:1000 for the anti-12S globulin antibody. The anti-12S globulin antibody was provided by I. Hara-Nishimura, and the anti-GST and anti-GFP

antibodies were purchased from Santa Cruz Biotechnology and Nacalai Tesque, respectively.

Crosslinking and Immunoprecipitation

Transgenic seedlings expressing GFP, GFP-tagged SAND1 or CCZ1a at 12 days of age were incubated with crosslink buffer [20 mM HEPES-KOH, 1% sucrose, and 1 mM dithiobis (succinimidyl propionate), pH 7.2] for 1 hour at RT, and Tris-HCl pH 7.5 was then added to 20 mM. The samples were then incubated for 10 min. Immunoprecipitation from detergent extracts was conducted using the micro-MACS GFP-tagged protein isolation kit (Miltenyi Biotec), according to the manufacturer's instructions.

Electron Microscopy

A. thaliana seeds were fixed with 4% paraformaldehyde (PFA) and 2% glutaraldehyde (GA) in 0.05 M cacodylate buffer, pH 7.4, at 4 °C overnight, which was followed by post-fixation with 2% osmium tetroxide (OsO4) in cacodylate buffer at 4 °C for 8 hours. The samples were then dehydrated in an ethanol series, infiltrated with propylene oxide, and embedded in Queol-651 resin (Nisshin EM). The samples were

ultra-thin-sectioned at 80 nm, stained with 2% uranyl acetate and lead stain solution (Sigma-Aldrich), and observed by transmission electron microscopy (JEM-1200EX; JEOL). For immunolabelling, *A. thaliana* seeds were fixed with 4% PFA, 0.1% GA, and 0.5% tannic acid in 0.05 M cacodylate buffer, pH 7.4, at 4 °C for 4 hours. The samples were then dehydrated through an ethanol series and embedded in LR white resin (London Resin). The samples were ultra-thin-sectioned at 80 nm, treated with the primary antibody diluted at 1:100 in PBS plus 1% BSA for 90 min at room temperature, incubated with the secondary antibody conjugated with gold particles (anti-rabbit IgG; British BioCell International) for 1 hour at room temperature, and fixed in 2% glutaraldehyde in 0.1 M phosphate buffer. The samples were then stained with 2% uranyl acetate and lead staining solution at room temperature.

Yeast Two-Hybrid Assay

The cDNAs for SAND1, CCZ1a, and CCZ1b were subcloned into pAD-GAL4-GWRFC or pBD-GAL4-GWRFC (provided by T. Demura). The plasmids were introduced into the AH109 strain (Clontech). Empty vectors were used as negative controls.

Coexpression and Purification of GST-tagged SAND1 and CCZ1

The open reading frame (ORF) for SAND1 was subcloned into the BamHI site in the multi cloning site (MCS) of the pGEX 4T-1 vector (GE Healthcare) to yield pGEX-SAND1. The ORFs for CCZ1a and CCZ1b were PCR-amplified and subcloned into the BamHI site in the MCS of the pQE-30 vector (Qiagen) to yield pQE-CCZ1a and pQE-CCZ1b. The DNA fragments containing the ribosome binding sites and the ORFs for His_6-CCZ1a and His_6-CCZ1b were PCR-amplified using pQE-CCZ1a or pQE-CCZ1b as a template and subcloned into the XhoI site in the MCS of pGEX-SAND1. GST-SAND1 and His_6-CCZ1a or His_6-CCZ1b were coexpressed in the *Escherichia coli* Rosetta strain. GST without SAND1 was used as a negative control. Cells expressing fusion proteins were collected and resuspended in lysis buffer (50 mM Tris, pH 8.0, 150 mM NaCl, and 1% Triton X-100) supplemented with a protease inhibitor cocktail (GE Healthcare), sonicated, and centrifuged at 16,000 ×*g* for 30 min. The supernatants were loaded onto a glutathione–Sepharose 4B column (GE Healthcare) and washed with washing buffer (50 mM Tris-HCl, pH 8.0, 150 mM NaCl, and 1% Triton X-100), and the fusion proteins were eluted with elution buffer (20 mM reduced glutathione, 50 mM Tris, pH 8.0, and 150 mM NaCl).

Nucleotide Exchange Assay Using Liposomes

RABG3f and ARA7 tagged with His_6 at the C-terminus were expressed in the *E. coli* Rosetta strain in the pET21a vector. Cells expressing the fusion protein were collected and resuspended in lysis buffer [50 mM Tris (pH 8.0), 150 mM NaCl, 0.5 mM $MgCl_2$, 1% Triton X-100, and protease inhibitor cocktail (GE Healthcare)], sonicated, and centrifuged at 16,000 ×*g* for 30 min. The supernatant was loaded onto a Ni-NTA His-Bind Resin column (Novagen) and washed with washing buffer [50 mM Tris (pH 8.0), 150 mM NaCl, 0.5 mM $MgCl_2$, and 1% Triton X-100], and then the fusion protein was eluted with elution buffer [200 mM imidazole, 50 mM Tris (pH 8.0), 150 mM NaCl, and 0.5 mM $MgCl_2$]. The GEF assay was performed as described by Cabrera et al. (2014). RABG3f-His_6 or ARA7-His_6 (500 pmol) was preloaded with MANT-GDP and incubated with 40 µl of liposomes at 11.5 mM consisting of 52.5% POPC (1-Palmitoyl-2-oleoyl-*sn*-glycero-3-phosphocholine), 30% DOGS-NTA (1,2-dioleoyl-sn-glycero-3-[N-5-amino-1-carboxylpentyl] iminodiacetic acid succinyl) (nickel salt), 10% PS (L-α-phosphatidylserine from porcine brain), and 7.5% PI3P [1,2-dihexadecanoyl-sn-glycero- 3-phospho-(1'-myo-inositol-3'-phosphate)] for 10 min at 25 °C. Then, the indicated amounts of SAND1-CCZ1 were added and incubated for 100 sec, and GMP-PNP was added to a final concentration of 0.1 mM to start the

nucleotide exchange reaction. MANT fluorescence was recorded using a fluorescence spectrophotometer (model F-2500, Hitachi High-technologies) at an excitation wavelength of 366 nm and an emission wavelength of 443 nm.

Accession Numbers

The Arabidopsis Genome Initiative locus identifiers for the genes mentioned in this article are At2g28390 (*SAND1*), At1g16020 (*CCZ1a*), At1g80910 (*CCZ1b*), At3g18820 (*RABG3f*), At5g45130 (*ARA7*), At5g45130 (*RHA1*), At3g54840 (*ARA6*), At3g19770 (*VPS9a*), At5g11150 (*VAMP713*) and At5g46860 (*SYP22*).

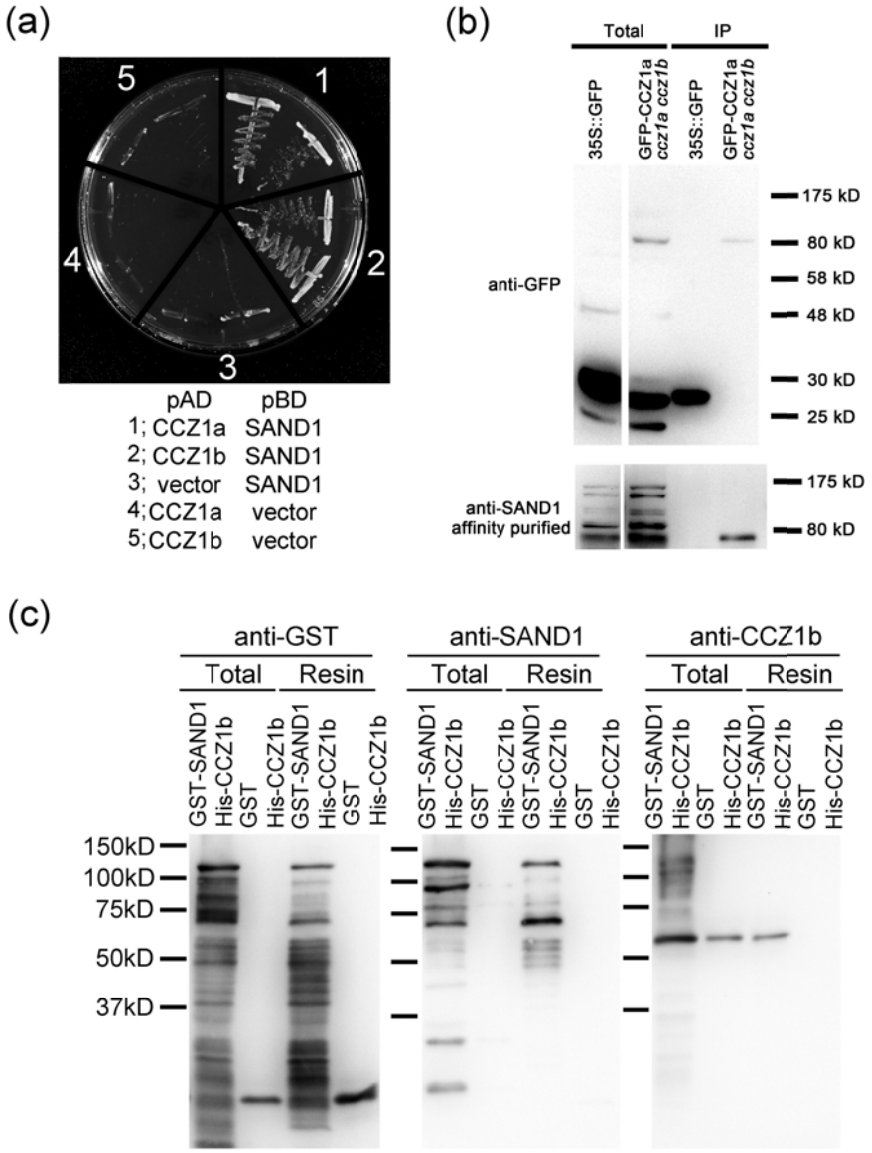

Figure 14 SAND1 and CCZ1 form a complex. (**a**) The interaction between SAND1 and CCZ1a/b was detected by the yeast-two-hybrid method. (b) SAND1 and CCZ1a form a complex in plants. Transgenic plants expressing GFP or GFP-CCZ1a were treated with the cross linker dithiobis (succinimidyl propionate), and GFP-tagged proteins were immunoprecipitated with the anti-GFP antibody from the lysates. Immunoprecipitates were subjected to immunoblotting with the anti-GFP antibody and the affinity-purified anti-SAND1 antibody. (**c**) His-tagged CCZ1b was co-purified with GS**T**-tagged SAND1 using glutathione sepharose from the lysate of *E. coli* co-expressing these proteins, indicating complex formation between SAND1 and CCZ1b.

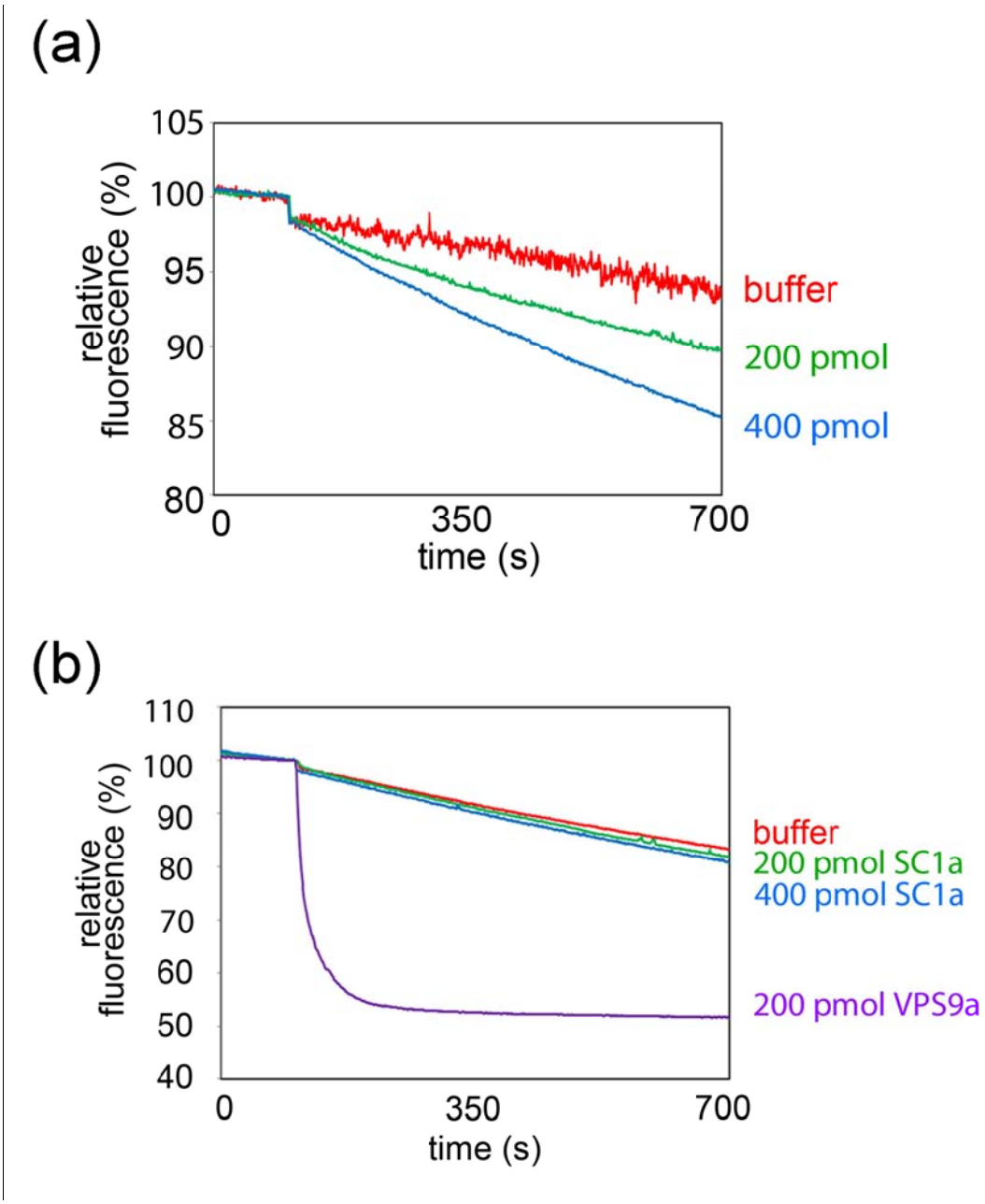

Figure 15 The SAND1-CCZ1a is the GEF of RABG3f/RAB7. (a) The SAND1-CCZ1 complex promoted nucleotide exchange on RAB7. Nucleotide exchange on RABG3f/RAB7 was measured in the absence (buffer) or presence of 200 pmol or 400 pmol of SAND1-CCZ1a. (**b)** The SAND1-CCZ1 complex did not exhibit significant GEF activity toward ARA7. Nucleotide exchange on ARA7 was measured in the absence (buffer) or presence of 200 pmol or 400 pmol of SAND1-CCZ1a (SC1a). Nucleotide exchange on ARA7 by 200 pmol of VPS9a was also measured as a positive control.

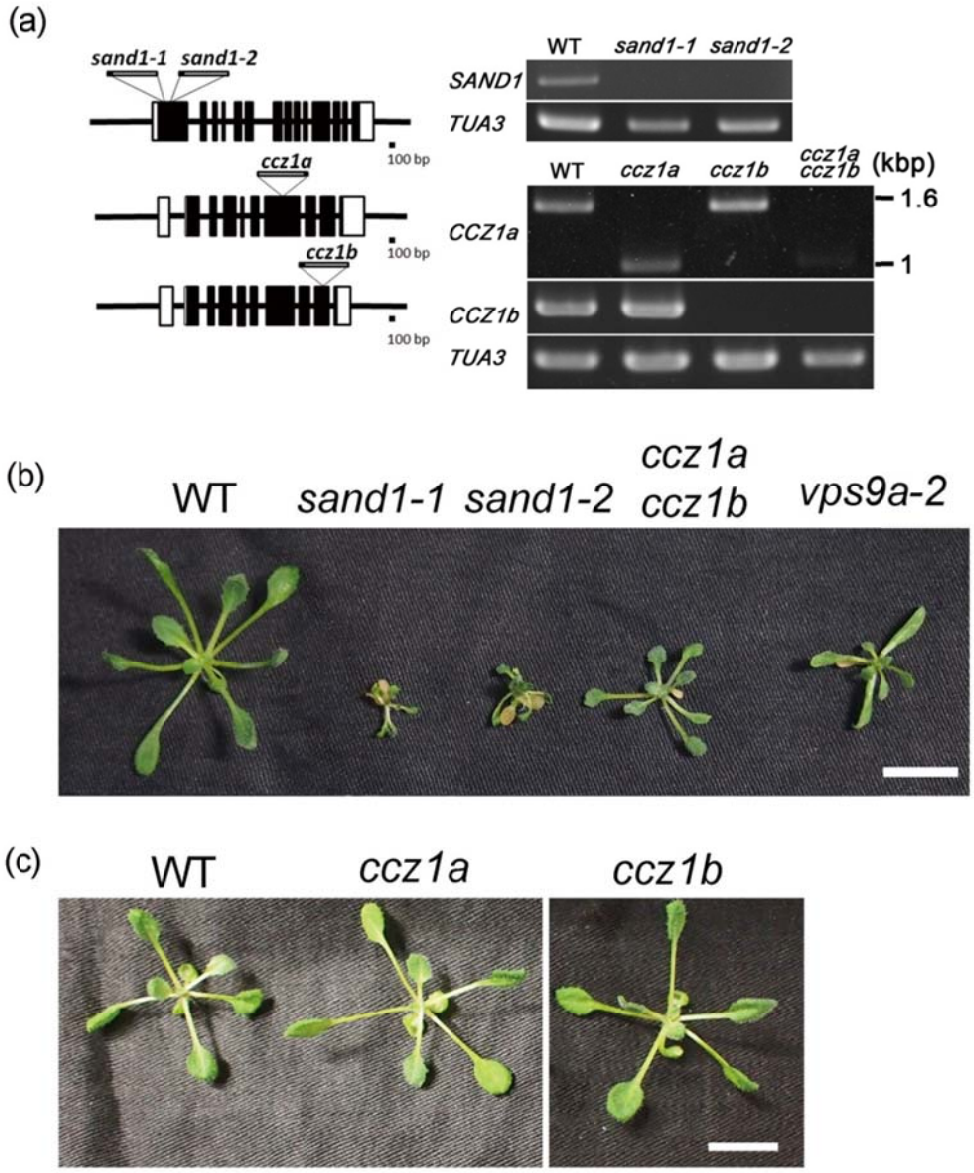

Figure 16 Both of two mutant alleles of *SAND1* showed a severe growth defect and the double mutant *ccz1a ccz1b* exhibited a slightly weaker growth defect. (**a**) Schematic representation of the gene structures of *SAND1*, *CCZ1a*, and *CCZ1b* and the T-DNA insertion site of each mutant. The absence of full-length transcripts was confirmed by RT-PCR. The 6th exon of *CCZ1a* (540 bp) did not exist in the transcript in the *ccz1a* mutant. (**b**) Phenotypes of *sand1* and *ccz1a ccz1b* double mutants. The *vps9a-2* mutant, which is defective in activation of RAB5 GTPases, is also presented. Bar = 1 cm. (**c**) The phenotypes of the *ccz1a* and *ccz1b* mutants were indistinguishable from that of the wild-type plant (WT). Bar = 1 cm.

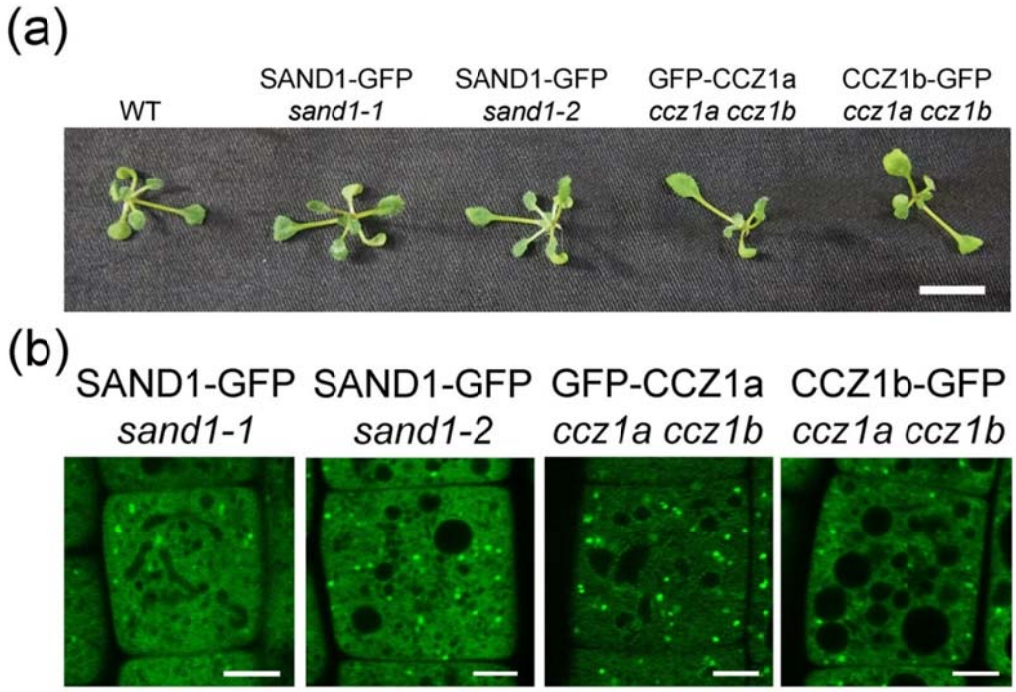

Figure 17 Fluorescently tagged proteins are functional and localize to the punctuate compartments and the cytosol. (**a**) The phenotypes of the *sand1* and *ccz1a ccz1b* mutants were restored by expression of GFP-tagged SAND1 or CCZ1 under the regulation of their own promoters. (**b**) Subcellular localization of SAND1 and CCZ1a/b. SAND1, CCZ1a, and CCZ1b were localized to punctate compartments and the cytosol. Bars = 5 μm.

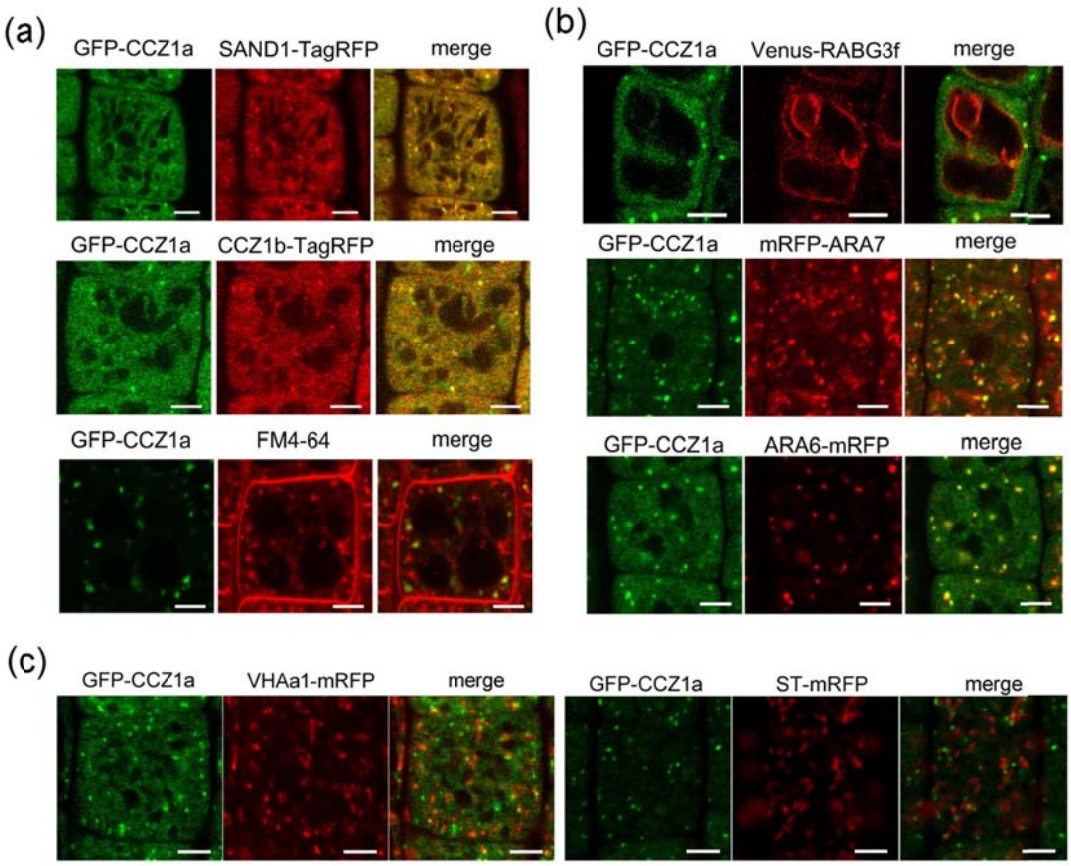

Figure 18 SAND1 and CCZ1a/b colocalize to endosomal compartments. They also colocalize with RAB5 and RAB7. (**a**) GFP-CCZ1a and SAND1-TagRFP expressed under the regulation of their own promoters colocalized to punctate compartments (upper panels). Colocalization between GFP-CCZ1a and CCZ1b-TagRFP was confirmed (middle panels). These punctate compartments were stained by FM4-64 after a 45 min incubation with 4 µM FM4-64, indicating their endosomal nature (lower panels). Bars = 5 µm. (**b**) Colocalization between CCZ1a and RAB5 or RABG3f/RAB7. GFP-CCZ1a partially colocalized with Venus-RABG3f (upper panels), and RAB5 (mRFP-ARA7 and ARA6-mRFP) exhibited better colocalization with CCZ1a (middle and lower panels). Bars = 5 µm. (**c**) Root epidermal cells of transgenic plants expressing GFP-CCZ1a and the TGN marker VHAa1-mRFP or the Golgi marker ST-mRFP. GFP-CCZ1a did not localize to the TGN or the Golgi. Bars = 5 µm.

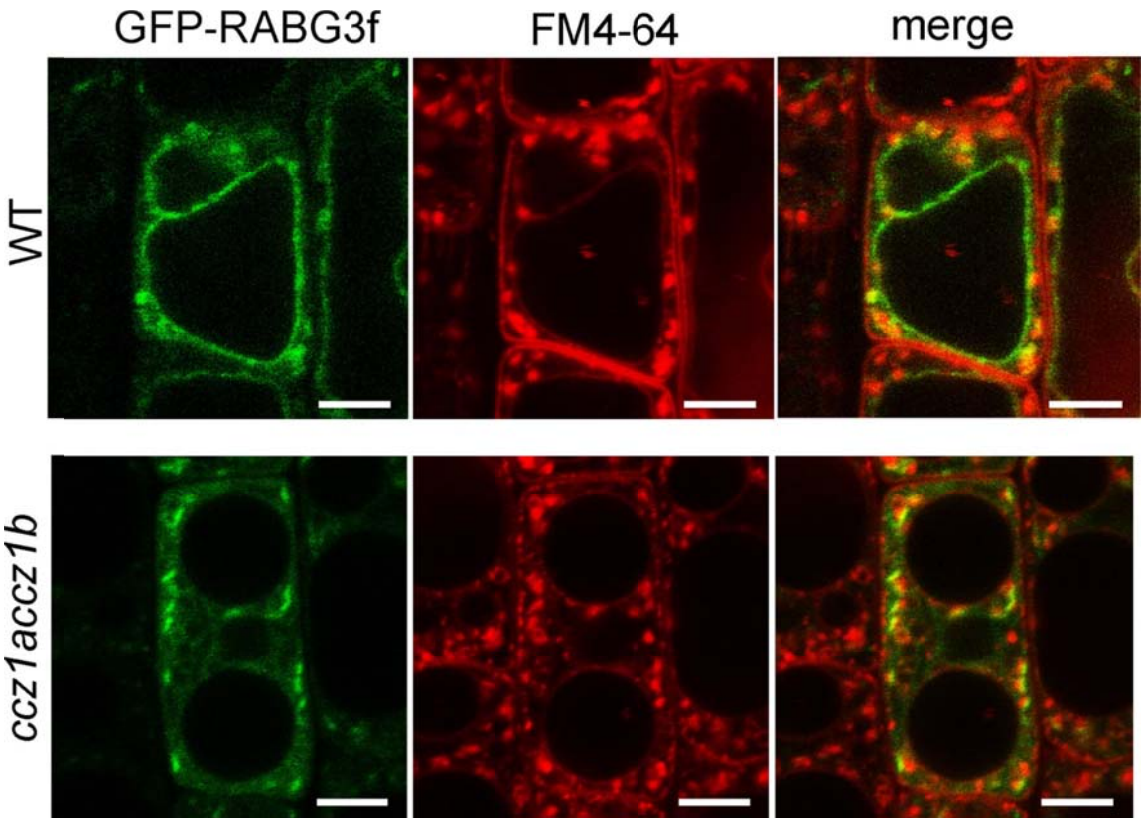

Figure 19 RAB7, which was localized to the vacuolar membrane and punctate compartments in wild-type plants (WT), failed to localize to the vacuolar membrane but localized to disc-like organelles in the *ccz1a ccz1b* double mutant. FM4-64 stained the punctate compartments, which were associated but not overlapping with the puncta bearing RABG3f in the *ccz1a ccz1b* double mutant. Bars = 5 μm.

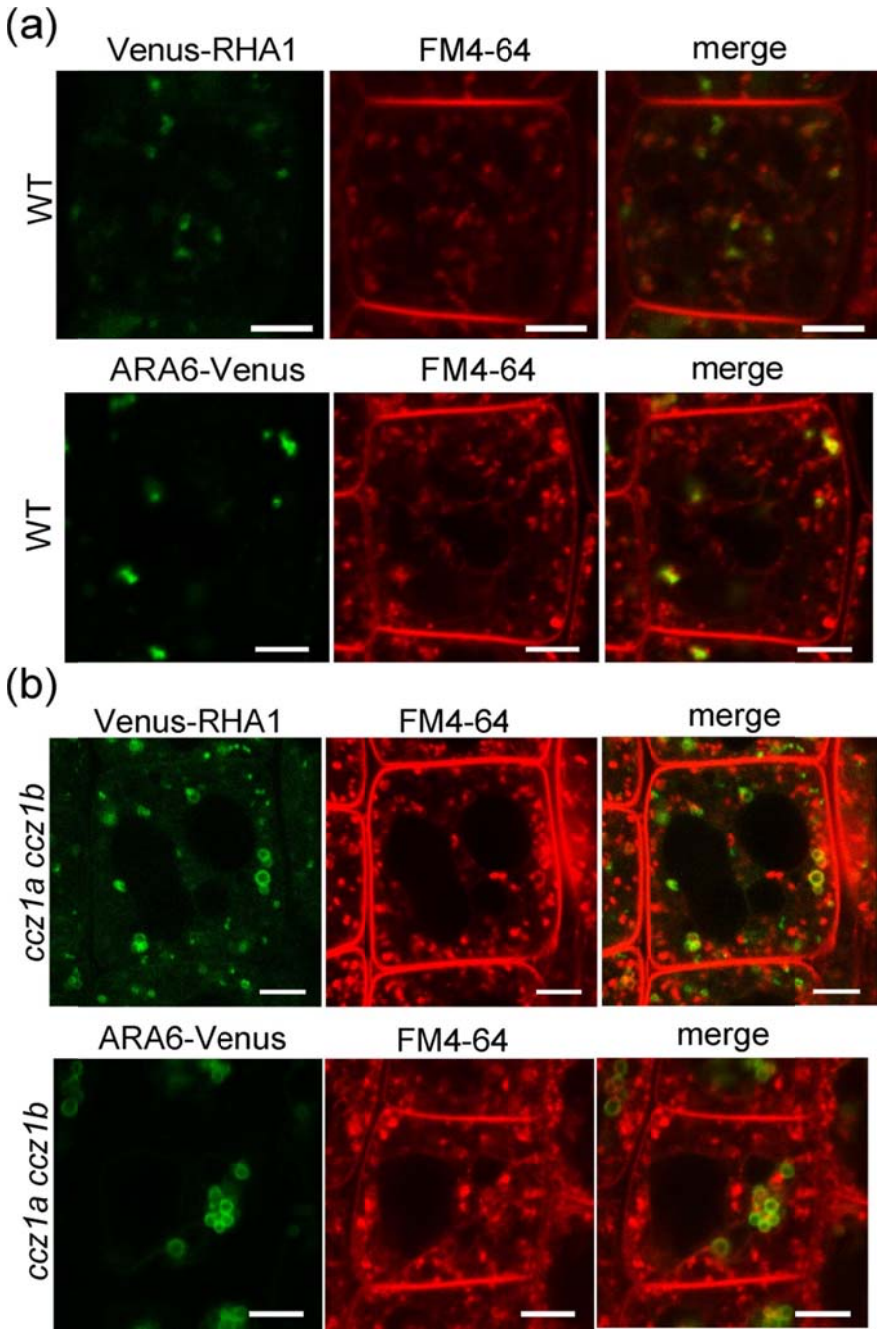

Figure 20 Sequential action of RAB5 and RAB7. (**a**) Root epidermal cells of transgenic plants expressing GFP-RHA1 or ARA6-GFP, which were labelled with FM4-64 and incubated for 45 min. Bars = 5 μm. **(b**) RAB5 (RHA1 or ARA6)-positive endosomes were dilated to form large ring-shaped structures, which were stained by FM4-64, indicating the endosomal property of these structures. The transport of the FM dye to the vacuolar membrane was not blocked. Bars = 5 μm.

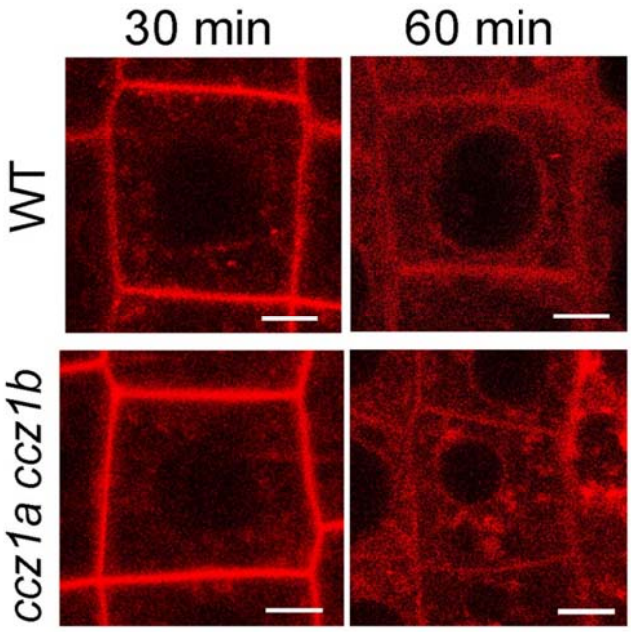

Figure 21 Endocytic membrane flow to the vacuole visualised by FM4-64. Root epidermal cells of wild-type and *ccz1a ccz1b* plants were stained with 4 μM FM4-64 for 30 or 60 min at RT. Bars = 5 μm.

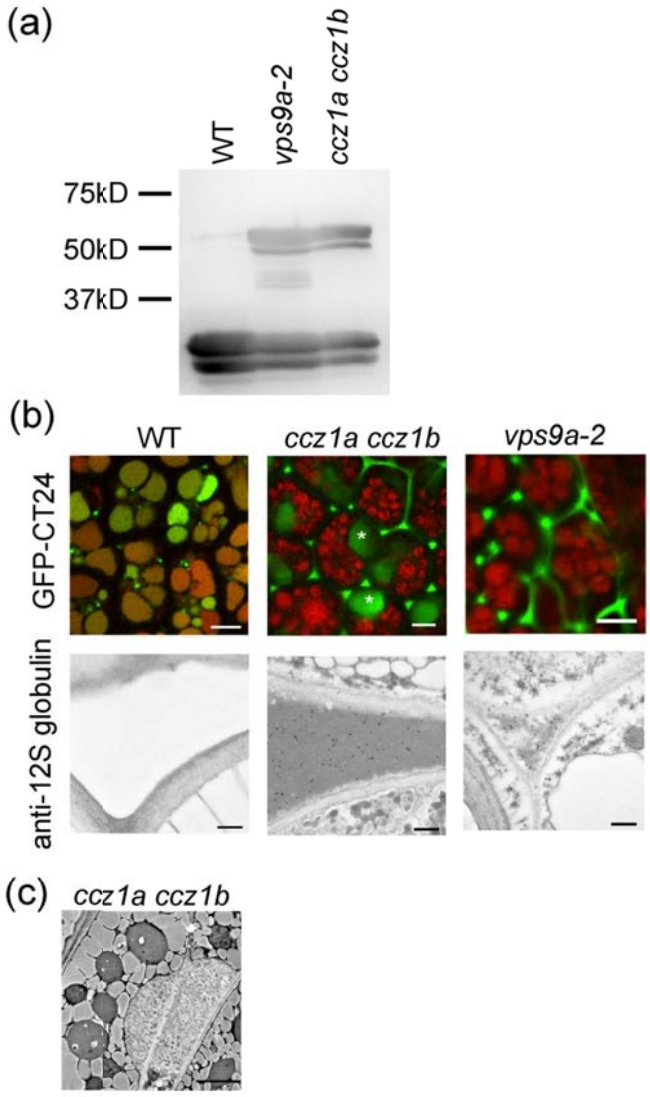

Figure 22 Transport and maturation of seed storage proteins is dependent on both RAB5 and RAB7. (a) Immunoblotting of seed proteins from wild-type (WT), *ccz1a ccz1b,* and *vps9a-2* mutant plants using the anti-12S globulin antibody. Precursors of 12S globulin accumulated in the both mutants. (**b**) GFP-CT24 was mis-secreted to the extracellular space in the *ccz1a ccz1b* and the *vps9a-2* mutants (upper panels). Immuno EM also demonstrated that 12S globulin is mis-secreted to the extracellular spaces in these mutants (lower panels). In addition to the typical accumulation pattern of mis-secreted proteins in the extracellular spaces observed in *vps9a-2*, large aggregating structures with GFP fluorescence were also observed in *ccz1a ccz1b* mutant embryos (asterisks). Bars = 5 μm (upper panels) and 0.5 μm (lower panels). (**c**) Large paramural bodies with numerous exosome-like vesicles were observed in *ccz1a ccz1b* mutant embryos by TEM. Bar = 2 μm.

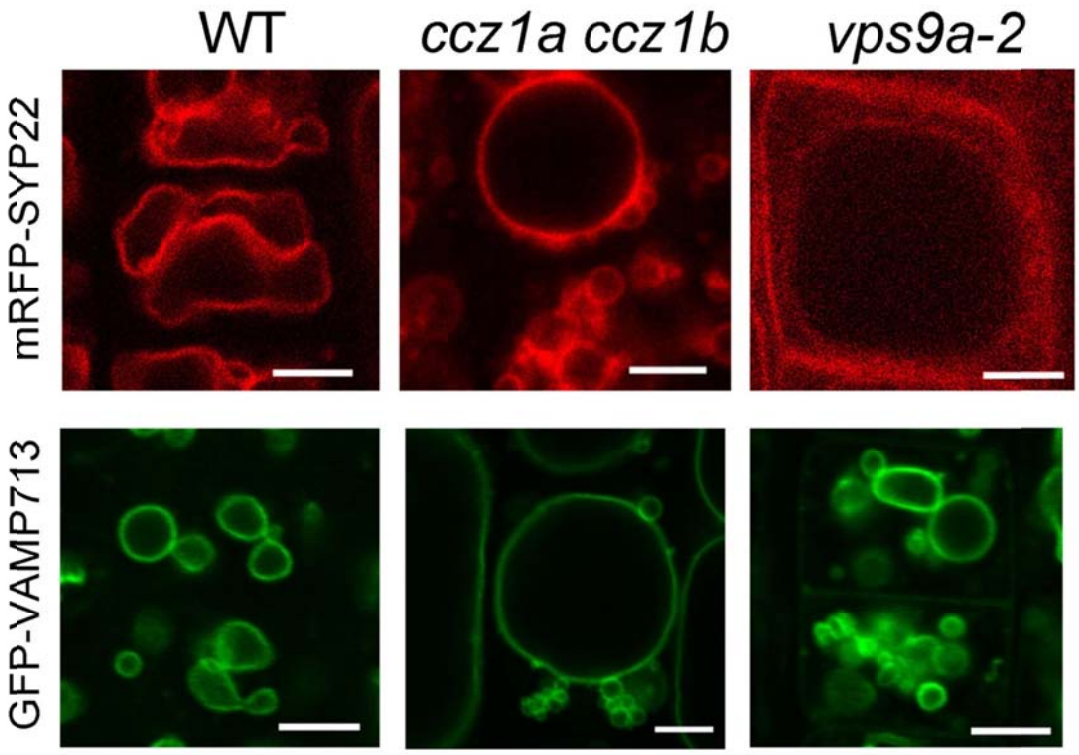

Figure 23 A membrane protein, SYP22, is transported to the tonoplast by a unique pathway regulated by RAB5 but not RAB7. Two SNARE proteins, SYP22 and VAMP713, are localized on vacuolar membranes in the epidermal cells of wild-type roots (left panels). While SYP22 is normally localized on the tonoplast in *ccz1a ccz1b*, it is substantially missecreted to the plasma membrane in *vps9a-2*. VAMP713 is also normally localized on the tonoplast in *ccz1a ccz1b*. In contrast to SYP22, the transport of VAMP713 to the vacuolar membranes is not so affected in *vps9a-2*. Bars = 5 μm.

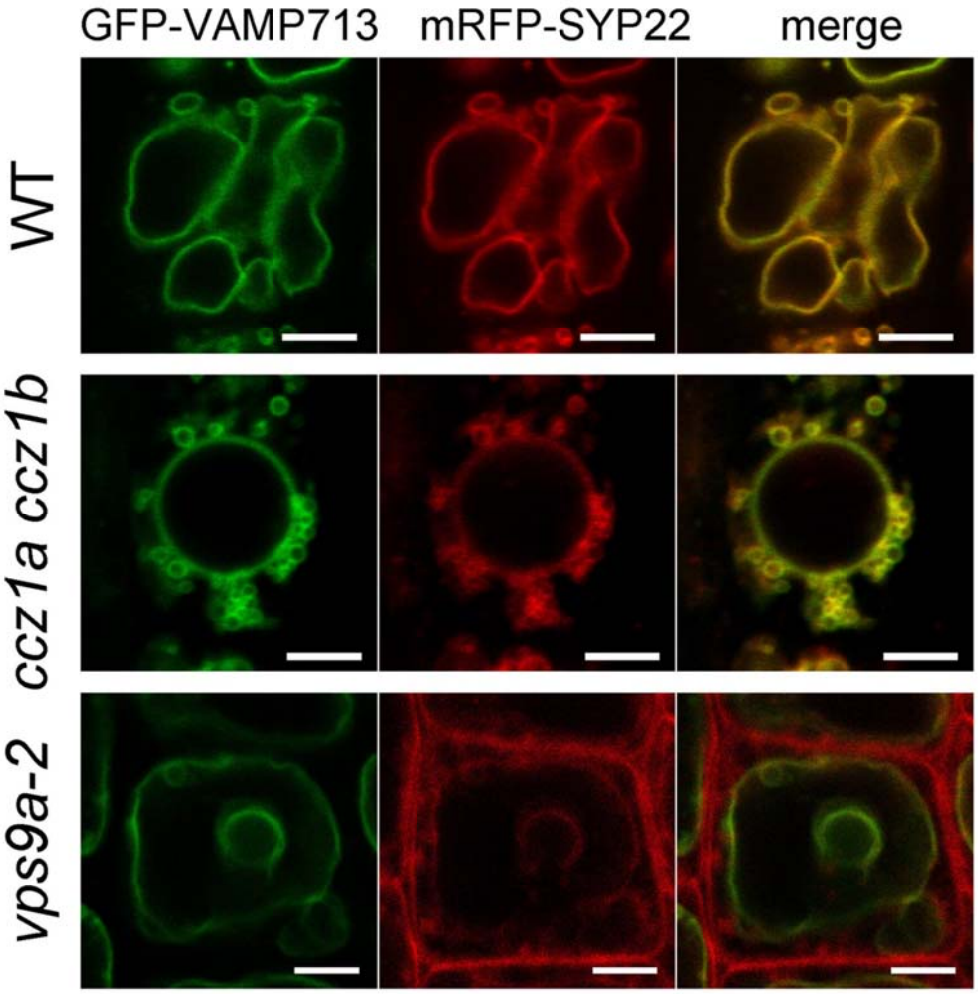

Figure 24 The unique pathway is ascertained by the observation of plant cells which coexpress two cargos which are delivered to the tonoplast in distinct ways. Root epidermal cells of wild-type (WT), *ccz1a ccz1b* and *vps9a-2* plants expressing both GFP-VAMP713 and mRFP-VAM3. Bars = 5 μm.

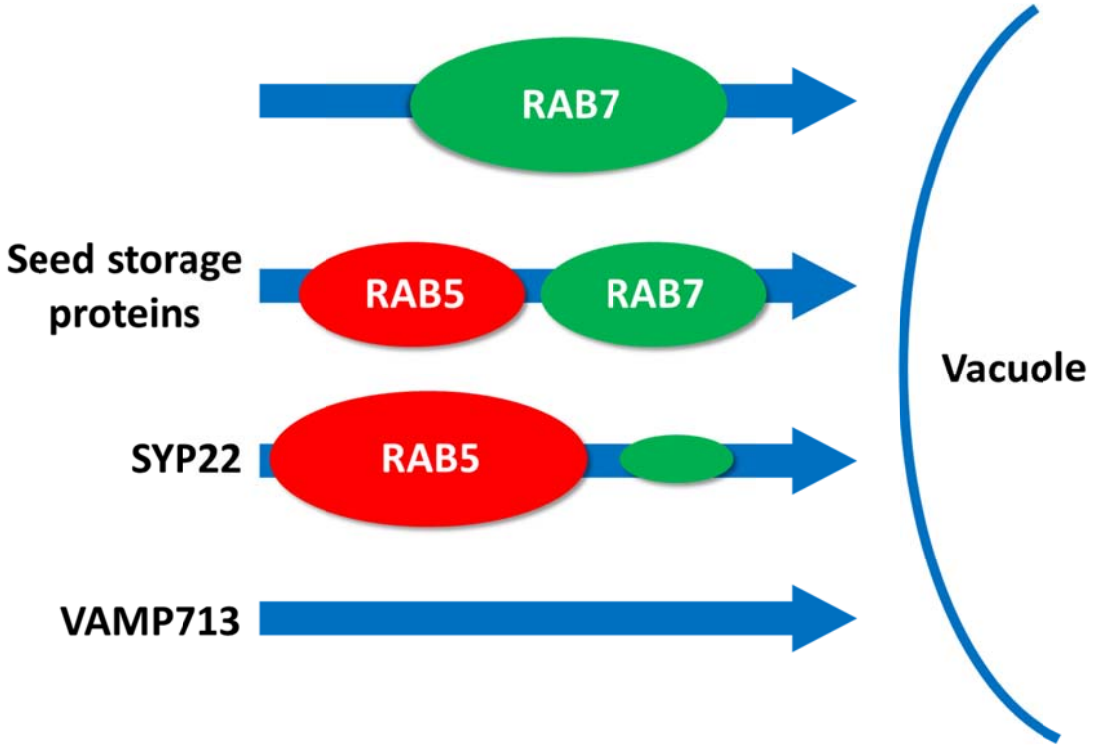

Figure 25 Model of multiple pathways to the vacuole in *Arabidopsis thaliana*. Seed storage proteins are transported to the vacuole in the pathway dependent on both RAB5 and RAB7. *A. thaliana* has a unique vacuolar pathway which is regulated by RAB5 but not RAB7. SYP22 is delivered to the tonoplast in this pathway. Trafficking of VAMP713 to the vacuole is dependent neither RAB5 nor RAB7.

General Discussion

In this study, I demonstrated significant roles of RAB5 activation at the tissue and organ levels. Some of the phenotypes such as defects in cell division, cell elongation, and morphogenesis could be caused by abnormal auxin distribution, which could be attributed to failure in transport and localization of PIN proteins to the target membranes. Thus, this study indicated the critical function of RAB5 in auxin-related developmental processes at cellular, tissue, and organ levels, which are related with each other. However, it still remains unknown how RAB5 activation is involved in *SHR* and *SCR* expression, which regulate root radial patterning. Analysis of SIEL in *vps9a-2* might reveal the molecular and cellular functions of RAB5 in ectopic periclinal division of the endodermis. Further detailed observation of the *vps9a-2* mutant could also lead to discovery of abnormalities other than those described above; analyses of such novel phenotypes are expected to result in finding of novel RAB5 functions at the molecular and cellular levels. It would be also effective to screen and analyze downstream effector molecules to reveal molecular and cellular functions of RAB5. Indeed, other members of my laboratory have discovered novel interesting proteins of conventional and plant-unique RAB5 members. VPS9a is a common activator for conventional and plant-specific RAB5 members. Conventional RAB5 regulates the vacuolar trafficking

pathway, and plant-unique ARA6 regulates the pathway from endosomes to the plasma membrane (Ebine *et al.* 2011). However, it also remains unclear which type of RAB5 takes part in localization of PIN and expression of *SHR* and *SCR*. Another interesting question is whether PIN4 localization on the plasma membrane, which is disturbed in the *vps9a-2* mutant, is regulated by ARA6, which regulates the trafficking pathway to the plasma membrane. PIN2 protein is likely transported to the vacuole by the action of conventional RAB5.

Regulation of vacuolar trafficking by RAB5 was further characterized in the Chapter 2, together with the function of RAB7. This study showed that *A. thaliana* has a unique trafficking route that is RAB5-dependent but independent of RAB7 in addition to the common vacuolar trafficking pathway where RAB5 and RAB7 act in a sequential manner. Seed storage proteins were indicated to be transported by the latter pathway, and SYP22, a SNARE protein, is transported via the former pathway. Furthermore, the analysis of VAMP713, another SNARE protein, raised two possibilities for the other vacuolar trafficking pathway. *A. thaliana* may have another pathway, which is not dependent on RAB5 or RAB7. Otherwise, VAMP713 may be able to reach the vacuolar membrane if either RAB5 or RAB7 is functional. Regarding the first possibility, it would be an interesting question to ask which RAB GTPase is responsible for this

trafficking pathway. To verify the second possibility, the analysis of the triple mutant, *vps9a-2 ccz1a ccz1b*, could be helpful. Another important question is which intermediate compartments are responsible for vacuolar transport of proteins analyzed in this study. It is widely investigated recently whether vacuolar proteins are delivered through the Golgi, trans-Golgi network, and endosomes in plants (Rojas-Pierce 2013, Xiang *et al.* 2013).

The function of RAB7 at the tissue and organ levels still remains as an open question, and comparison of the RAB7 function with the RAB5 function described in Chapter 1 would be helpful to understand the higher-order functions of common and unique trafficking pathways, which plants have acquired through evolution.

References

Achard, P., Gusti, A., Cheminant, S., Alioua, M., Dhondt, S., Coppens, F., Beemster, G.T. and Genschik, P. (2009) Gibberellin signaling controls cell proliferation rate in Arabidopsis. *Current biology* **19**, 1188-1193.

Ackers, J.P., Dhir, V. and Field, M.C. (2005) A bioinformatic analysis of the RAB genes of Trypanosoma brucei. *Molecular and biochemical parasitology*, **141**, 89-97.

Aida, M., Beis, D., Heidstra, R., Willemsen, V., Blilou, I., Galinha, C., Nussaume, L., Noh, Y.S., Amasino, R. and Scheres, B. (2004) The PLETHORA genes mediate patterning of the Arabidopsis root stem cell niche. *Cell*, **119**, 109-120.

Alonso, J.M., Stepanova, A.N., Leisse, T.J., Kim, C.J., Chen, H., Shinn, P., Stevenson, D.K., Zimmerman, J., Barajas, P., Cheuk, R., Gadrinab, C., Heller, C., Jeske, A., Koesema, E., Meyers, C.C., Parker, H., Prednis, L., Ansari, Y., Choy, N., Deen, H., Geralt, M., Hazari, N., Hom, E., Karnes, M., Mulholland, C., Ndubaku, R., Schmidt, I., Guzman, P., Aguilar-Henonin, L., Schmid, M., Weigel, D., Carter, D.E., Marchand, T., Risseeuw, E., Brogden, D., Zeko, A., Crosby, W.L., Berry, C.C. and Ecker, J.R. (2003) Genome-wide insertional mutagenesis of Arabidopsis thaliana. *Science*, **301**, 653-657.

Barr, F.A. (2013) Review series: Rab GTPases and membrane identity: causal or inconsequential? *The Journal of cell biology*, **202**, 191-199.

Beck, M., Zhou, J., Faulkner, C., Maclean, D. and Robatzek, S. (2012) Spatio-Temporal Cellular Dynamics of the Arabidopsis Flagellin Receptor Reveal Activation Status-Dependent Endosomal Sorting. *The Plant cell*, **10**, 4205-4219.

Benfey, P.N. and Scheres, B. (2000) Root development. *Current biology*, **10**, R813-815.

Blilou, I., Xu, J., Wildwater, M., Willemsen, V., Paponov, I., Friml, J., Heidstra, R., Aida, M., Palme, K. and Scheres, B. (2005) The PIN auxin efflux facilitator network controls growth and patterning in Arabidopsis roots. *Nature*, **433**, 39-44.

Bohdanowicz, M. and Grinstein, S. (2010) Vesicular traffic: a Rab SANDwich. *Current biology*, **20**, R311-314.

Bolte, S., Lanquar, V., Soler, M.N., Beebo, A., Satiat-Jeunemaitre, B., Bouhidel, K. and Thomine, S. (2011) Distinct lytic vacuolar compartments are embedded inside the protein storage vacuole of dry and germinating Arabidopsis thaliana seeds. *Plant & cell physiology*, **52**, 1142-1152.

Bottanelli, F., Foresti, O., Hanton, S. and Denecke, J. (2011) Vacuolar transport in tobacco leaf epidermis cells involves a single route for soluble cargo and multiple routes for membrane cargo. *The Plant cell*, **23**, 3007-3025.

Bottanelli, F., Gershlick, D.C. and Denecke, J. (2012) Evidence for sequential action of Rab5 and Rab7 GTPases in prevacuolar organelle partitioning. *Traffic*, **13**, 338-354.

Brady, S.M., Orlando, D.A., Lee, J.Y., Wang, J.Y., Koch, J., Dinneny, J.R., Mace, D., Ohler, U. and Benfey, P.N. (2007) A high-resolution root spatiotemporal map reveals dominant expression patterns. *Science*, **318**, 801-806.

Cabrera, M., Nordmann, M., Perz, A., Schmedt, D., Gerondopoulos, A., Barr, F., Piehler, J., Engelbrecht-Vandre, S. and Ungermann, C. (2014) The Mon1-Ccz1 GEF activates the Rab7 GTPase Ypt7 via a longin fold-Rab interface and association with PI-3-P-positive membranes. *Journal of cell science*, in press.

Choi, S.W., Tamaki, T., Ebine, K., Uemura, T., Ueda, T. and Nakano, A. (2013) RABA members act in distinct steps of subcellular trafficking of the Flagellin Sensing2 receptor. *The Plant cell*, **25**, 1174-1187.

Cui, H., Levesque, M.P., Vernoux, T., Jung, J.W., Paquette, A.J., Gallagher, K.L., Wang, J.Y., Blilou, I., Scheres, B. and Benfey, P.N. (2007) An evolutionarily conserved mechanism delimiting SHR movement defines a single layer of endodermis in plants. *Science*, **316**, 421-425.

Dacks, J.B. and Field, M.C. (2007) Evolution of the eukaryotic membrane-trafficking system: origin, tempo and mode. *Journal of cell science*, **120**, 2977-2985.

Dacks, J.B., Poon, P.P. and Field, M.C. (2008) Phylogeny of endocytic components yields insight into the process of nonendosymbiotic organelle evolution. *Proceedings of the National Academy of Sciences of the United States of America*, **105**, 588-593.

De Marcos Lousa, C., Gershlick, D.C. and Denecke, J. (2012) Mechanisms and concepts paving the way towards a complete transport cycle of plant vacuolar sorting receptors. *The Plant cell*, **24**, 1714-1732.

Dhonukshe, P., Tanaka, H., Goh, T., Ebine, K., Mahonen, A.P., Prasad, K., Blilou, I., Geldner, N., Xu, J., Uemura, T., Chory, J., Ueda, T., Nakano, A., Scheres, B. and Friml, J. (2008) Generation of cell polarity in plants links endocytosis, auxin distribution and cell fate decisions. *Nature*, **456**, 962-966.

Ebine, K., Fujimoto, M., Okatani, Y., Nishiyama, T., Goh, T., Ito, E., Dainobu, T., Nishitani, A., Uemura, T., Sato, M.H., Thordal-Christensen, H., Tsutsumi, N., Nakano, A. and Ueda, T. (2011) A membrane trafficking pathway regulated by the plant-specific RAB GTPase ARA6. *Nature cell biology*, **13**, 853-859.

Ebine, K., Miyakawa, N., Fujimoto, M., Uemura, T., Nakano, A. and Ueda, T. (2012) Endosomal trafficking pathway regulated by ARA6, a RAB5 GTPase unique to plants. *Small GTPases*, **3**, 23-27.

Ebine, K., Okatani, Y., Uemura, T., Goh, T., Shoda, K., Niihama, M., Morita, M.T., Spitzer, C.,

Otegui, M.S., Nakano, A. and Ueda, T. (2008) A SNARE complex unique to seed plants is required for protein storage vacuole biogenesis and seed development of Arabidopsis thaliana. *The Plant cell*, **20**, 3006-3021.

Ebine, K. and Ueda, T. (2009) Unique mechanism of plant endocytic/vacuolar transport pathways. *Journal of plant research*, **122**, 21-30.

Ferreira, P.C., Hemerly, A.S., Engler, J.D., van Montagu, M., Engler, G. and Inze, D. (1994) Developmental expression of the arabidopsis cyclin gene cyc1At. *The Plant cell*, **6**, 1763-1774.

Field, M.C., Natesan, S.K., Gabernet-Castello, C. and Koumandou, V.L. (2007) Intracellular trafficking in the trypanosomatids. *Traffic*, **8**, 629-639.

Friml, J., Benkova, E., Blilou, I., Wisniewska, J., Hamann, T., Ljung, K., Woody, S., Sandberg, G., Scheres, B., Jurgens, G. and Palme, K. (2002a) AtPIN4 mediates sink-driven auxin gradients and root patterning in Arabidopsis. *Cell*, **108**, 661-673.

Friml, J., Vieten, A., Sauer, M., Weijers, D., Schwarz, H., Hamann, T., Offringa, R. and Jurgens, G. (2003) Efflux-dependent auxin gradients establish the apical-basal axis of Arabidopsis. *Nature*, **426**, 147-153.

Friml, J., Wisniewska, J., Benkova, E., Mendgen, K. and Palme, K. (2002b) Lateral relocation of auxin efflux regulator PIN3 mediates tropism in Arabidopsis. *Nature*, **415**, 806-809.

Fuji, K., Shimada, T., Takahashi, H., Tamura, K., Koumoto, Y., Utsumi, S., Nishizawa, K., Maruyama, N. and Hara-Nishimura, I. (2007) Arabidopsis vacuolar sorting mutants (green fluorescent seed) can be identified efficiently by secretion of vacuole-targeted green fluorescent protein in their seeds. *The Plant cell*, **19**, 597-609.

Gao, X.Q., Li, C.G., Wei, P.C., Zhang, X.Y., Chen, J. and Wang, X.C. (2005) The dynamic changes of tonoplasts in guard cells are important for stomatal movement in Vicia faba. *Plant physiology*, **139**, 1207-1216.

Geldner, N., Anders, N., Wolters, H., Keicher, J., Kornberger, W., Muller, P., Delbarre, A., Ueda, T., Nakano, A. and Jurgens, G. (2003) The Arabidopsis GNOM ARF-GEF mediates endosomal recycling, auxin transport, and auxin-dependent plant growth. *Cell*, **112**, 219-230.

Goh, T., Uchida, W., Arakawa, S., Ito, E., Dainobu, T., Ebine, K., Takeuchi, M., Sato, K., Ueda, T. and Nakano, A. (2007) VPS9a, the common activator for two distinct types of Rab5 GTPases, is essential for the development of Arabidopsis thaliana. *The Plant cell*, **19**, 3504-3515.

Grieneisen, V.A., Xu, J., Maree, A.F., Hogeweg, P. and Scheres, B. (2007) Auxin transport is sufficient to generate a maximum and gradient guiding root growth. *Nature*, **449**,

1008-1013.

Grosshans, B.L., Ortiz, D. and Novick, P. (2006) Rabs and their effectors: achieving specificity in membrane traffic. *Proceedings of the National Academy of Sciences of the United States of America*, **103**, 11821-11827.

Hamaji, K., Nagira, M., Yoshida, K., Ohnishi, M., Oda, Y., Uemura, T., Goh, T., Sato, M.H., Morita, M.T., Tasaka, M., Hasezawa, S., Nakano, A., Hara-Nishimura, I., Maeshima, M., Fukaki, H. and Mimura, T. (2009) Dynamic aspects of ion accumulation by vesicle traffic under salt stress in Arabidopsis. *Plant & cell physiology*, **50**, 2023-2033.

Hatsugai, N., Iwasaki, S., Tamura, K., Kondo, M., Fuji, K., Ogasawara, K., Nishimura, M. and Hara-Nishimura, I. (2009) A novel membrane fusion-mediated plant immunity against bacterial pathogens. *Genes & development*, **23**, 2496-2506.

Heidstra, R., Welch, D. and Scheres, B. (2004) Mosaic analyses using marked activation and deletion clones dissect Arabidopsis SCARECROW action in asymmetric cell division. *Genes & development*, **18**, 1964-1969.

Helariutta, Y., Fukaki, H., Wysocka-Diller, J., Nakajima, K., Jung, J., Sena, G., Hauser, M.T. and Benfey, P.N. (2000) The SHORT-ROOT gene controls radial patterning of the Arabidopsis root through radial signaling. *Cell*, **101**, 555-567.

Jaillais, Y., Santambrogio, M., Rozier, F., Fobis-Loisy, I., Miege, C. and Gaude, T. (2007) The retromer protein VPS29 links cell polarity and organ initiation in plants. *Cell*, **130**, 1057-1070.

Kinchen, J.M. and Ravichandran, K.S. (2010) Identification of two evolutionarily conserved genes regulating processing of engulfed apoptotic cells. *Nature*, **464**, 778-782.

Kleine-Vehn, J., Leitner, J., Zwiewka, M., Sauer, M., Abas, L., Luschnig, C. and Friml, J. (2008) Differential degradation of PIN2 auxin efflux carrier by retromer-dependent vacuolar targeting. *Proceedings of the National Academy of Sciences of the United States of America*, **105**, 17812-17817.

Koizumi, K., Wu, S., MacRae-Crerar, A. and Gallagher, K.L. (2011) An essential protein that interacts with endosomes and promotes movement of the SHORT-ROOT transcription factor. *Current biology*, **21**, 1559-1564.

Kremer, K., Kamin, D., Rittweger, E., Wilkes, J., Flammer, H., Mahler, S., Heng, J., Tonkin, C.J., Langsley, G., Hell, S.W., Carruthers, V.B., Ferguson, D.J. and Meissner, M. (2013) An overexpression screen of Toxoplasma gondii Rab-GTPases reveals distinct transport routes to the micronemes. *PLoS pathogens*, **9**, e1003213.

Kubo, M., Udagawa, M., Nishikubo, N., Horiguchi, G., Yamaguchi, M., Ito, J., Mimura, T., Fukuda, H. and Demura, T. (2005) Transcription switches for protoxylem and

metaxylem vessel formation. *Genes & development*, **19**, 1855-1860.

Limpens, E., Ivanov, S., van Esse, W., Voets, G., Fedorova, E. and Bisseling, T. (2009) Medicago N2-fixing symbiosomes acquire the endocytic identity marker Rab7 but delay the acquisition of vacuolar identity. *The Plant cell*, **21**, 2811-2828.

Lincoln, C., Britton, J.H. and Estelle, M. (1990) Growth and development of the axr1 mutants of Arabidopsis. *The Plant cell*, **2**, 1071-1080.

Mackiewicz, P. and Wyroba, E. (2009) Phylogeny and evolution of Rab7 and Rab9 proteins. *BMC evolutionary biology*, **9**, 101.

Marty, F. (1999) Plant vacuoles. *The Plant cell*, **11**, 587-600.

Matsuzaki, M., Misumi, O., Shin, I.T., Maruyama, S., Takahara, M., Miyagishima, S.Y., Mori, T., Nishida, K., Yagisawa, F., Yoshida, Y., Nishimura, Y., Nakao, S., Kobayashi, T., Momoyama, Y., Higashiyama, T., Minoda, A., Sano, M., Nomoto, H., Oishi, K., Hayashi, H., Ohta, F., Nishizaka, S., Haga, S., Miura, S., Morishita, T., Kabeya, Y., Terasawa, K., Suzuki, Y., Ishii, Y., Asakawa, S., Takano, H., Ohta, N., Kuroiwa, H., Tanaka, K., Shimizu, N., Sugano, S., Sato, N., Nozaki, H., Ogasawara, N., Kohara, Y. and Kuroiwa, T. (2004) Genome sequence of the ultrasmall unicellular red alga Cyanidioschyzon merolae 10D. *Nature*, **428**, 653-657.

Mizuno-Yamasaki, E., Rivera-Molina, F. and Novick, P. (2012) GTPase networks in membrane traffic. *Annual review of biochemistry*, **81**, 637-659.

Mo, B., Tse, Y.C. and Jiang, L. (2006) Plant prevacuolar/endosomal compartments. *International review of cytology*, **253**, 95-129.

Muller, A., Guan, C., Galweiler, L., Tanzler, P., Huijser, P., Marchant, A., Parry, G., Bennett, M., Wisman, E. and Palme, K. (1998) AtPIN2 defines a locus of Arabidopsis for root gravitropism control. *EMBO J*, **17**, 6903-6911.

Nakada-Tsukui, K., Saito-Nakano, Y., Husain, A. and Nozaki, T. (2010) Conservation and function of Rab small GTPases in Entamoeba: annotation of E. invadens Rab and its use for the understanding of Entamoeba biology. *Experimental parasitology*, **126**, 337-347.

Nakajima, K., Sena, G., Nawy, T. and Benfey, P.N. (2001) Intercellular movement of the putative transcription factor SHR in root patterning. *Nature*, **413**, 307-311.

Niihama, M., Takemoto, N., Hashiguchi, Y., Tasaka, M. and Morita, M.T. (2009) ZIP genes encode proteins involved in membrane trafficking of the TGN-PVC/vacuoles. *Plant & cell physiology*, **50**, 2057-2068.

Nimchuk, Z.L., Tarr, P.T., Ohno, C., Qu, X. and Meyerowitz, E.M. (2011) Plant stem cell signaling involves ligand-dependent trafficking of the CLAVATA1 receptor kinase. *Current biology*, **21**, 345-352.

Nishizawa, K., Maruyama, N., Satoh, R., Fuchikami, Y., Higasa, T. and Utsumi, S. (2003) A C-terminal sequence of soybean beta-conglycinin alpha' subunit acts as a vacuolar sorting determinant in seed cells. *The Plant journal : for cell and molecular biology*, **34**, 647-659.

Paciorek, T., Zazimalova, E., Ruthardt, N., Petrasek, J., Stierhof, Y.D., Kleine-Vehn, J., Morris, D.A., Emans, N., Jurgens, G., Geldner, N. and Friml, J. (2005) Auxin inhibits endocytosis and promotes its own efflux from cells. *Nature*, **435**, 1251-1256.

Paquette, A.J. and Benfey, P.N. (2005) Maturation of the ground tissue of the root is regulated by gibberellin and SCARECROW and requires SHORT-ROOT. *Plant physiology*, **138**, 636-640.

Pedrazzini, E., Komarova, N.Y., Rentsch, D. and Vitale, A. (2013) Traffic routes and signals for the tonoplast. *Traffic*, **14**, 622-628.

Pereira-Leal, J.B. (2008) The Ypt/Rab family and the evolution of trafficking in fungi. *Traffic*, **9**, 27-38.

Poteryaev, D., Datta, S., Ackema, K., Zerial, M. and Spang, A. (2010) Identification of the switch in early-to-late endosome transition. *Cell*, **141**, 497-508.

Rink, J., Ghigo, E., Kalaidzidis, Y. and Zerial, M. (2005) Rab conversion as a mechanism of progression from early to late endosomes. *Cell*, **122**, 735-749.

Robatzek, S., Chinchilla, D. and Boller, T. (2006) Ligand-induced endocytosis of the pattern recognition receptor FLS2 in Arabidopsis. *Genes & development*, **20**, 537-542.

Rojas-Pierce, M. (2013) Targeting of tonoplast proteins to the vacuole. *Plant science : an international journal of experimental plant biology*, **211**, 132-136.

Rojo, E., Gillmor, C.S., Kovaleva, V., Somerville, C.R. and Raikhel, N.V. (2001) VACUOLELESS1 is an essential gene required for vacuole formation and morphogenesis in Arabidopsis. *Developmental cell*, **1**, 303-310.

Rosso, M.G., Li, Y., Strizhov, N., Reiss, B., Dekker, K. and Weisshaar, B. (2003) An Arabidopsis thaliana T-DNA mutagenized population (GABI-Kat) for flanking sequence tag-based reverse genetics. *Plant molecular biology*, **53**, 247-259.

Sabatini, S., Beis, D., Wolkenfelt, H., Murfett, J., Guilfoyle, T., Malamy, J., Benfey, P., Leyser, O., Bechtold, N., Weisbeek, P. and Scheres, B. (1999) An auxin-dependent distal organizer of pattern and polarity in the Arabidopsis root. *Cell*, **99**, 463-472.

Sabatini, S., Heidstra, R., Wildwater, M. and Scheres, B. (2003) SCARECROW is involved in positioning the stem cell niche in the Arabidopsis root meristem. *Genes & development*, **17**, 354-358.

Saito, C., Morita, M.T., Kato, T. and Tasaka, M. (2005) Amyloplasts and vacuolar membrane dynamics in the living graviperceptive cell of the Arabidopsis inflorescence stem.

The Plant cell, **17**, 548-558.

Saito, C. and Ueda, T. (2009) Chapter 4: functions of RAB and SNARE proteins in plant life. *International review of cell and molecular biology*, **274**, 183-233.

Sanmartin, M., Ordonez, A., Sohn, E.J., Robert, S., Sanchez-Serrano, J.J., Surpin, M.A., Raikhel, N.V. and Rojo, E. (2007) Divergent functions of VTI12 and VTI11 in trafficking to storage and lytic vacuoles in Arabidopsis. *Proceedings of the National Academy of Sciences of the United States of America*, **104**, 3645-3650.

Sarkar, A.K., Luijten, M., Miyashima, S., Lenhard, M., Hashimoto, T., Nakajima, K., Scheres, B., Heidstra, R. and Laux, T. (2007) Conserved factors regulate signalling in Arabidopsis thaliana shoot and root stem cell organizers. *Nature*, **446**, 811-814.

Sauer, M. and Kleine-Vehn, J. (2011) AUXIN BINDING PROTEIN1: the outsider. *The Plant cell*, **23**, 2033-2043.

Sena, G., Jung, J.W. and Benfey, P.N. (2004) A broad competence to respond to SHORT ROOT revealed by tissue-specific ectopic expression. *Development*, **131**, 2817-2826.

Shirakawa, M., Ueda, H., Shimada, T., Nishiyama, C. and Hara-Nishimura, I. (2009) Vacuolar SNAREs function in the formation of the leaf vascular network by regulating auxin distribution. *Plant & cell physiology*, **50**, 1319-1328.

Spitzer, C., Reyes, F.C., Buono, R., Sliwinski, M.K., Haas, T.J. and Otegui, M.S. (2009) The ESCRT-related CHMP1A and B proteins mediate multivesicular body sorting of auxin carriers in Arabidopsis and are required for plant development. *The Plant cell*, **21**, 749-766.

Takano, J., Miwa, K., Yuan, L., von Wiren, N. and Fujiwara, T. (2005) Endocytosis and degradation of BOR1, a boron transporter of Arabidopsis thaliana, regulated by boron availability. *Proceedings of the National Academy of Sciences of the United States of America*, **102**, 12276-12281.

Tamura, K., Shimada, T., Ono, E., Tanaka, Y., Nagatani, A., Higashi, S.I., Watanabe, M., Nishimura, M. and Hara-Nishimura, I. (2003) Why green fluorescent fusion proteins have not been observed in the vacuoles of higher plants. *The Plant journal : for cell and molecular biology*, **35**, 545-555.

Ubeda-Tomas, S., Federici, F., Casimiro, I., Beemster, G.T., Bhalerao, R., Swarup, R., Doerner, P., Haseloff, J. and Bennett, M.J. (2009) Gibberellin signaling in the endodermis controls Arabidopsis root meristem size. *Current biology*, **19**, 1194-1199.

Ueda, T., Uemura, T., Sato, M.H. and Nakano, A. (2004) Functional differentiation of endosomes in Arabidopsis cells. *The Plant journal : for cell and molecular biology*, **40**, 783-789.

Ueda, T., Yamaguchi, M., Uchimiya, H. and Nakano, A. (2001) Ara6, a plant-unique novel

type Rab GTPase, functions in the endocytic pathway of Arabidopsis thaliana. *EMBO J*, **20**, 4730-4741.

Uejima, T., Ihara, K., Goh, T., Ito, E., Sunada, M., Ueda, T., Nakano, A. and Wakatsuki, S. (2010) GDP-bound and nucleotide-free intermediates of the guanine nucleotide exchange in the Rab5.Vps9 system. *J Biol Chem*, **285**, 36689-36697.

Uejima, T., Ihara, K., Sunada, M., Kawasaki, M., Ueda, T., Kato, R., Nakano, A. and Wakatsuki, S. (2013) Direct metal recognition by guanine nucleotide-exchange factor in the initial step of exchange reaction. *Acta Cryst. D. in press*.

Ulmasov, T., Murfett, J., Hagen, G. and Guilfoyle, T.J. (1997) Aux/IAA proteins repress expression of reporter genes containing natural and highly active synthetic auxin response elements. *The Plant cell*, **9**, 1963-1971.

Vieten, A., Vanneste, S., Wisniewska, J., Benkova, E., Benjamins, R., Beeckman, T., Luschnig, C. and Friml, J. (2005) Functional redundancy of PIN proteins is accompanied by auxin-dependent cross-regulation of PIN expression. *Development*, **132**, 4521-4531.

Welch, D., Hassan, H., Blilou, I., Immink, R., Heidstra, R. and Scheres, B. (2007) Arabidopsis JACKDAW and MAGPIE zinc finger proteins delimit asymmetric cell division and stabilize tissue boundaries by restricting SHORT-ROOT action. *Genes & development*, **21**, 2196-2204.

Wysocka-Diller, J.W., Helariutta, Y., Fukaki, H., Malamy, J.E. and Benfey, P.N. (2000) Molecular analysis of SCARECROW function reveals a radial patterning mechanism common to root and shoot. *Development*, **127**, 595-603.

Xiang, L., Etxeberria, E. and Van den Ende, W. (2013) Vacuolar protein sorting mechanisms in plants. *The FEBS journal*, **280**, 979-993.

Xu, T., Wen, M., Nagawa, S., Fu, Y., Chen, J.G., Wu, M.J., Perrot-Rechenmann, C., Friml, J., Jones, A.M. and Yang, Z. (2010) Cell surface- and rho GTPase-based auxin signaling controls cellular interdigitation in Arabidopsis. *Cell*, **143**, 99-110.